Aalto University
School of Chemical
Technology

School of Chemical Technology
Degree Programme of Bioproducts Technology

Ville Rissanen

PROCESS OPTIMIZATION OF CELLULOSE FIBRIL PRODUCTION - THE EFFECT OF PROCESS MEDIUM COMPOSITION ON ENERGY EFFICIENCY AND PRODUCT QUALITY

Master's thesis for the degree of Master of Science in Technology submitted for inspection, Espoo, September 12, 2016.

Supervisor **Professor Olli Dahl**

Instructors **D.Sc. Jari Sirviö, M.Sc. Panu Lahtinen**

Aalto University
School of Chemical
Technology

Aalto University, P.O. BOX 11000, 00076 AALTO
www.aalto.fi

Abstract of master's thesis

Author	Ville Rissanen
Title of thesis	Process optimization of cellulose fibril production – The effect of process medium composition on energy efficiency and product quality
Department	Department of Forest Products Technology
Professorship	Environmental Management
Code of professorship	Puu-127
Thesis supervisor	Professor Olli Dahl
Thesis advisor(s)	D.Sc. Jari Sirviö, M.Sc. Panu Lahtinen
Date	12.09.2016
Number of pages	58+10
Language	English

Abstract

Cellulosic nanomaterials are a new family of renewable biomaterials that have the potential to widely expand the application range of cellulose fibres. For this reason, they have been under extensive research over the last decade. The purpose of this Master's thesis was to provide an outlook on the process optimization of mechanical processing of cellulose nanofibrils, focusing on the composition of the process medium. More precisely, the effects of the process medium on the energy efficiency and product quality of cellulose fibril production were studied.

The effect of the process medium was studied by comparing the fibrillation of never-dried birch kraft pulp dispersed in reverse osmosis water, tap water and a 5 % dose of a green additive. Three additives were tested: glycerol, a Prosoft debonder solution and a choline chloride – glycerol (1:2) deep eutectic solvent (DES). Prior to processing, the pulp was ion-exchanged to the sodium counter-ion form with optimal swelling and fibrillation conditions. A Masuko friction grinder was used for the fibrillation. To assess the quality of the fibrillated materials, their properties were analysed with a combination of characterization methods chosen from literature. The results of the characterization methods were presented as a function of specific net energy consumption to illustrate the relation between energy efficiency and product quality for each sample.

The results from the characterization methods consistently demonstrated that reverse osmosis water provided the best fibrillation results, especially at lower energy levels. The effect of glycerol was negligible, while the divalent cations in tap water disrupted the swelling of fibres and their subsequent fibrillation. The deep eutectic solvent behaved similarly as tap water, implying it does not retain its complex form in aqueous solutions but reverts to a halide salt and glycerol, the former of which disrupts the fibrillation similarly as the ions in tap water. The fibres dispersed in the debonder solution showed the weakest results overall, and their behaviour suggests the fibrils form flocks around the cationic polymers of the debonder solution, heavily disrupting their fibrillation and the formation of an interfibrillar network. Finally, the quality parameters of the fibrils peak between net energy levels 2 and 3 kWh/kg for all mediums except the debonder solution. This indicates that prolonged grinding reduces the aspect ratio of the fibrils, resulting in weakening of the fibril network.

Keywords Fibrillated cellulose, mechanical fibrillation, energy efficiency, process medium, fibre swelling properties, viscosity, transmittance, water retention

Tekijä Ville Rissanen

Työn nimi Selluloosafibrillien tuotantoprosessin optimointi – väliaineen koostumuksen vaikutus tuotannon energiatehokkuuteen ja lopputuotteen laatuun

Laitos Puunjalostustekniikan laitos

Professuuri Ympäristöasioiden hallinta **Professuurikodi** Puu-127

Työn valvoja Prof. Olli Dahl

Työn ohjaaja(t) MMT Jari Sirviö, DI Panu Lahtinen

Päivämäärä 12.09.2016 **Sivumäärä** 58+10 **Kieli** englanti

Tiivistelmä

Selluloosananomateriaalit ovat joukko uusiutuvia biomateriaaleja, jotka voivat merkittävästi lisätä selluloosakuitujen sovellusmahdollisuuksia. Tästä syystä ne ovat olleet laajalti tutkittuja viimeisen vuosikymmenen ajan. Tämä diplomityö pyrkii tarjoamaan tuoreen näkökulman selluloosafibrillien mekaanisen tuotantoprosessin systemaattiseen optimointiin. Työssä tutkittiin prosessiväliaineen koostumuksen vaikutusta fibrillien tuotannon energiankulutukseen ja syntyvän lopputuotteen laatuun.

Prosessiväliaineen vaikutusta tutkittiin vertaamalla Kraft-putkisellun (koivu) fibrillaatiota joko käänteisosmoosiveteen, hanaveteen, tai 5 % vahvuiseen vihreään lisäaineeseen dispergoituna. Työssä testattiin kolmea eri lisäainetta: glyserolia, Prosoft–debonderia, sekä koliinikloridi-glyseroli (1:2) syväeutektista liuotinta (DES). Ennen mekaanista prosessointia Masuko -jauhimella kuitu pestiin natrium-vastaionimuotoon, mikä parantaa sen turpoamis- ja fibrilloitumisominaisuuksia. Fibrilloidun materiaalin laadun arviointiin käytettiin kirjallisuudesta valikoituja karakterisointimenetelmiä. Menetelmien tulokset esitettiin spesifisen nettoenergiankulutuksen funktiona prosessin energiatehokkuuden ja näytteiden laadun välisen suhteen havainnollistamiseksi.

Karakterisointimenetelmien tulokset osoittivat johdonmukaisesti, että käänteisosmoosivesi mahdollisti kuitujen tehokkaimman fibrillaation etenkin alhaisemmilla jauhatusenergiatasoilla. Glyserolin lisäyksen vaikutus jäi mitättömäksi, mutta hanaveden divalenttien kationeiden todettiin häiritsevän kuitujen turpoamista ja sitä kautta niiden fibrilloitumista. Syväeutektisen liuottimen vaikutus oli samankaltainen kuin hanavedellä, antaen ymmärtää että sen kompleksirakenne hajoaa vesiliuoksessa takaisin halidisuolaksi ja glyseroliksi, joista ensin mainittu häiritsee kuitujen fibrillaatiota samoin kuin hanaveden kationit. Prosoft-debonderiliuokseen dispergoidut kuidut saivat heikoimmat tulokset kaikissa karakterisointimenetelmissä. Niiden käyttäytymisestä pääteltiin kuitujen muodostavan flokkeja kationisen debonderipolymeerin ympärille, mikä heikentää kuitujen fibrillaatiota, sekä fibrilliverkkorakenteen muodostumista. Debonderinäytettä lukuun ottamatta kaikkien näytteiden laatuparametrit saavuttivat huippunsa noin 2-3 kWh/kg:n energiatason kohdalla. Tämä viittaa siihen, että pidempään jatkuva jauhatus pienentää kuitujen muotosuhdetta, joka puolestaan heikentää fibrillien muodostaman verkkorakenteen vahvuutta.

Avainsanat Fibrilloitu selluloosa, mekaaninen fibrillaatio, energiatehokkuus, prosessiväliaine, kuidun turpoaminen, viskositeetti, transmittanssi, vesiretentio

PREFACE

This Master's thesis was carried out at VTT Technical Research Centre of Finland in the Biomass processing technologies group. During this work I had the pleasure to be acquainted with a number of pleasant and helpful persons, to whom I would like to extend a warm acknowledgement.

Firstly, I would like to thank Professor Kristiina Kruus and Jari Sirviö for allowing me the opportunity to work on this project, and for their guidance and feedback on matters large and small. Similarly, I would like to thank Professor Olli Dahl for looking after me as my supervisor, and Panu Lahtinen for his continuous readiness to provide me with insights, tutoring and feedback as my advisor. Many thanks are due to Jari Leino for instructing me with the use of the Masuko friction grinder, Ulla Salonen and Katja Pettersson for instructing me with the characterization procedures and providing me with the optical microscopy images, and Asko Sneck for the SEM images. Also, Juhani Tuomi from Solenis is acknowledged for providing us with the Prosoft debonder.

Espoo, June 7, 2016

Ville Rissanen

TABLE OF CONTENTS

LIST OF ABBREVIATIONS

AFM	atomic force microscopy
BC	bacterial cellulose
BET	Brunauer – Emmet – Teller
CMC	carboxymethyl cellulose
CNC	cellulose nanocrystals
CNF	cellulose nanofibrils
DES	deep eutectic solvent
DMSO	dimethyl sulfoxide
DP	degree of polymerization
G’	storage modulus
G’’	loss modulus
GRW	gravimetric water retention
FE-SEM	field-emission scanning electron microscopy
LbL	layer-by-layer
LD-PE	low density polyethylene
MFC	microfibrillated cellulose
NaBr	sodium bromide
$NaHCO_3$	sodium bicarbonate
NaOCl	sodium hydrochlorite
NaOH	sodium hydroxide
NMR	nuclear magnetic resonance
OM	optical microscopy
Pd	palladium
PE	polyethylene
PET	polyethylene terephthalate
PLA	polylactic acid
PP	polypropylene
Pt	platinum
PVOH	polyvinyl alcohol
RO	reverse osmosis
SAXS	small-angle X-ray scattering
SEM	scanning electron microscopy
SSA	specific surface area
TAPPI	technical association of the pulp and paper industry
TEM	transmission electron microscopy
TEMPO	2,2,6,6-Tetramethylpiperidine-1-oxyl
XRD	X-ray diffraction
YMC	yield multiplier constant

1. INTRODUCTION

With the ever-improving understanding of human-induced environmental issues of the past, present and the future, the concepts of environmentalism and sustainability have gained an increasing amount of attention and support during the last few decades. After the 2015 United Nations Climate Change Conference, it seems that reducing the environmental impacts of human activity has finally been, at least tentatively, acknowledged as a global high-priority concern (Tollefson & Weiss 2015). Furthermore, the development of green technology and utilization of renewable resources has been emphasized as a means to advance towards environmental sustainability (Goodland 1995).

The utilization of renewable resources can be divided into two categories: renewable energy and renewable materials. Of these, the pursuit to find renewable energy sources has gained a lot of attention as the means to combat climate change, but the use of renewable materials is also crucial to curb pollution and exhaustion of our planet's resources. The most important renewable material in our possession is undoubtedly cellulose. Cellulose is the most abundant biopolymer in the world, and its versatile properties have allowed to be utilized as a source of fuel, as well as raw material for building, clothing and recording information on (Klemm et al. 2005).

In the more recent years the advances in the mechanical and chemical processing of cellulose have led to the development of cellulose nanomaterials, which can further broaden the variety of cellulose-based applications (Klemm et al. 2011). As the name suggests, cellulose nanomaterials have at least one dimension in the nanometer range, and they can be extracted from cellulosic fibres by mechanical, chemical or enzymatic means. Of these, cellulose nanofibrils (CNF) are long, thin and branched fibril fragments isolated from fibres through mechanical fibrillation. They possess a high aspect ratio and specific surface area, which enables them to form a strong fibre-fibre network that gives CNF their unique properties (Kangas et al. 2014).

CNF has potential in a wide variety of applications ranging from reinforcing elements in lightweight materials to rheology modifiers in emulsions or structural components of transparent films (Shatkin et al. 2014), but the major drawback of large-scale CNF production has traditionally been its high energy consumption. Although a number of chemical and enzymatic pre-treatments have been developed to facilitate CNF production and improve its properties, there is still much room for systematic process optimization. This thesis aims to contribute to this end by researching the relations between process conditions, energy consumption and product quality of CNF production via a friction grinder. The focus in this work is on the ionic composition of the process water and the use of ionic and non-ionic green additives as a pre-treatment.

2. LITERATURE REVIEW

2.1 Cellulose and nanocellulose

2.1.1. Cellulose

Cellulose is one of the most significant natural polymers available to mankind throughout its history. Mainly originating from wood, cotton, hemp and other plant-based materials, cellulose and its derivatives are renewable, biodegradable, biocompatible and virtually inexhaustible, making them attractive sources of sustainable raw materials on an industrial scale (Klemm et al. 2005). Abdul Khalil et al. (2012) reported that approximately 7.5 x 10^{10} tonnes of cellulose are processed annually.

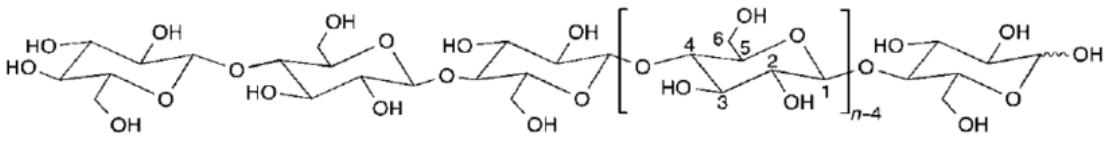

Figure 1. Molecular structure of cellulose (Nishiyama et al. 2003)

The structure and properties of cellulose have been thoroughly investigated since its discovery in 1883. As seen in figure 1, cellulose is a carbohydrate polymer consisting of a linear chain of repeating monosaccharides, namely β(1→4) linked D-glucose units (Klemm et al. 2005). The amount of glucose units, i.e. the degree of polymerization (DP) varies with the origin of the raw material and the nature of possible treatment, typically from several hundred (wood pulp) to more than a ten thousand (cotton fibres) (Habibi 2014).

Figure 2 shows the formation of the hierarchal structure of a cellulosic polymer in a plant cell wall. In this process the individual cellulose chains, or fibrils, aggregate into a repeated structure with amorphous and crystalline regions to form microfibrils, which further aggregate into macroscopic fibres (Eichhorn et al. 2010).

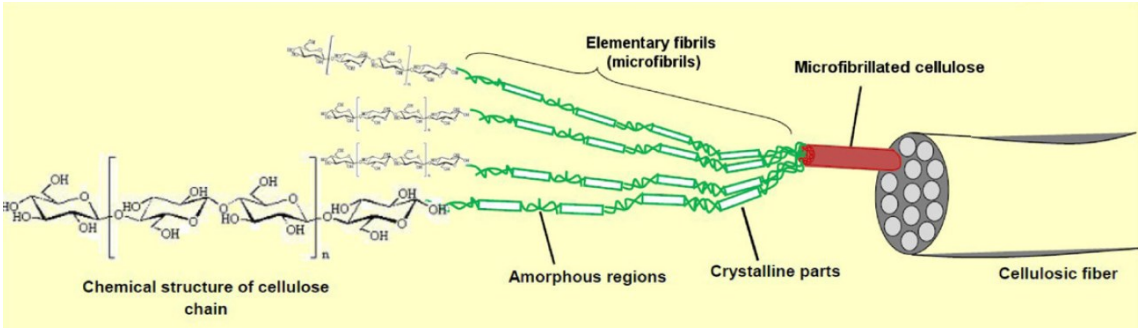

Figure 2. The hierarchical structure of a cellulosic fibre (Lavoine et al. 2012).

The large amount of hydroxyl groups, three in each monomer, in cellulose polymers creates a hydrogen bond network that makes cellulose a relatively stable polymer that exhibits high axial stiffness, has no melting point and is insoluble to typical aqueous solvents. The hydroxyl groups are also very reactive, giving the polymer high functionality and modification (Eichhorn et al. 2010).

Cellulose exists in four different polymorphs: cellulose I, II, III and IV. Cellulose I is also called native cellulose, as it is the primary source of cellulosic materials. It occurs in two allomorphs, I_α and I_β. Cellulose II, also called regenerated cellulose as it emerges

through sodium hydroxide (NaOH) regeneration, is the most stabile crystalline form of cellulose. Polymorphs III and IV are formed from celluloses I and II with subsequent treatments (Lavoine et al. 2012). Practically all cellulosic materials discussed in this thesis are in the cellulose I form.

2.1.2. Cellulosic nanomaterials

Besides the more traditional methods of utilizing cellulose, the isolation and utilization of nano-scale cellulose fibres, or cellulosic nanomaterials, have gained remarkable attention during the last decade.

By definition, cellulosic nanomaterials are cellulose fibrils with at least one outer dimension at nanoscale (1-100nm). They possess all the properties of regular cellulosic materials mentioned above, but due to their small size and large specific surface area their reactivity and ability to form bonds and create networks is increased even further (Klemm et al. 2011). These properties create possibilities to utilize cellulose nanomaterials in a wide variety of applications in both old and new fields of product development, as discussed in further chapters.

Cellulosic nanomaterials can be divided into four distinct categories by their size, characteristics and method of preparation: cellulose microfibrils (CMF), cellulose nanofibrils (CNF), cellulose nanocrystals (CNC) and bacterial cellulose (BC) (Klemm et al. 2011). This thesis is concerned with the processing of cellulose nanofibrils.

2.1.3. Cellulose nanofibrils

Cellulose nanofibrils (CNF) are nano-scaled units isolated from cellulose fibres using mechanical shearing forces that cause fibrillation, i.e. lateral delamination of the fibres into their sub-structures (nanofibrils) with diameter in the range of 10-40 nm and length of several micrometres (Habibi 2014).

The manufacturing of CNF was first implemented by Turbak et al. (1985) in the late 70s and early 80s. They created gel-like material by homogenizing wood-based cellulose suspensions with high pressure and called it microfibrillated cellulose (MFC). Since then, the nomenclature of nanocellulose has been rather ununiform, and a variety of

terms are still being used to refer to the material. However, the Technical Association of the Pulp and Paper Industry (TAPPI) has proposed to standardize the terminology concerning cellulose nanomaterials (Standard Terms and Their Definition for Cellulose Nanomaterial WI 3021). Herein, the term “cellulose nanofibrils” (CNF), are used as per this proposal.

Despite the remarkable potential of CNF, its commercial development was hindered for more than two decades due to two manufacturing issues. Firstly, the homogenizer was easily clogged by the fibres, resulting in frequent maintenance breaks and thus inconsistent production rate. Secondly, the traditional production process of CNF requires multiple passes through the homogenizer unit, consuming considerable amounts of energy – more than 25 000 kWh per ton of CNF (Klemm et al. 2011). These issues raised the production costs to unfeasible levels, hence holding back further research at the time.

During the 2000s, however, the growing interest in renewable materials resulted in the revival of CNF research, which also resulted in the development of more efficient production technologies that have led to a wide variety of commercially successful or promising applications (Shatkin et al. 2014). In addition with thousands of patents and other publications there are currently several commercial-scale CNF production facilities around the world, as well an increasing number of semi-commercial and pilot-scale facilities. Moreover, there are dozens of lab scale research projects focusing on CNF production and applications (Kangas 2014).

2.2. Production of cellulose nanofibrils

2.2.1. Mechanical processing

The production of cellulose nanofibrils is implemented by fibrillating cellulose fibres into nano-scale particles with intense mechanical treatment. For this purpose, a number of methods and equipment have been developed, the most prevalent of

which are based on homogenization, microfluidization and grinding (Spence et al. 2011). The basic operating principles of these methods are demonstrated in figure 3.

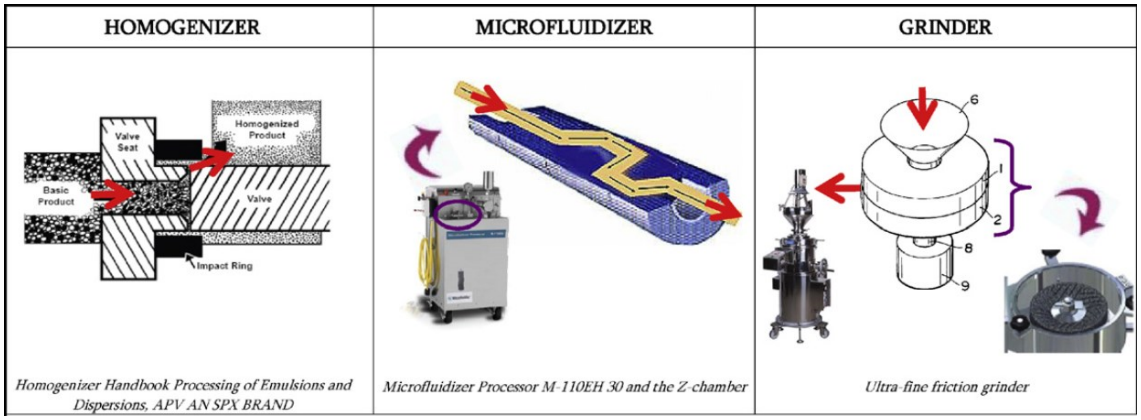

Figure 3. The operating principles of the most common mechanical treatment processes for cellulose nanofibril production: the homogenizer, the microfluidizer and the grinder (Lavoine et al. 2012).

Homogenization of cellulose was the pioneering method for the production of cellulose nanofibres. In this method dilute fibre-water –suspension is forced through a narrow slit using high pressure, where it is consequently subjected to rapid pressure drops and shear forces that induce a high degree of fibrillation on the fibres (Lavoine et al. 2012; Spence et al. 2011). The main issue with this method is that multiple passes through the homogenizer unit (10-20 passes) are required for the raw material to fully fibrillate into gel-like nanofibrils, making the process remarkably energy-intensive (Osong et al. 2015). Moreover, the long cellulose fibres easily clog the system due to the presence of moving parts around the high-pressure valve (Spence et al. 2011). To prevent this drawback it is necessary to reduce the size of fibres before homogenization (Abdul Khalil et al. 2014).

A more novel way to perform homogenization is to utilize microfluidizers, in which the pulp is fed through a z-shaped interaction chamber under high pressure, causing defibrillation of the fibres through impacts, collisions and shear forces against the channel walls and colliding streams. A lesser number of cycles through the fluidizer (5-20 cycles) are enough to produce CNF compared to traditional homogenizing, decreasing the overall energy consumption. Additionally, this method decreases the

likelihood of clogging due to the absence of moving parts, and also provides more uniformly sized fibres compared to homogenizer. Clogging of unpretreated fibres is still an issue, however, and during microfluidizing the clogs can only be cleared by halting the process and applying reverse flow (Abdul Khalil et al. 2014; Spence et al. 2011).

The third frequently used method for CNF production is grinding, commonly performed with Masuko ultra-fine friction grinders. During this process, wood fibres are forced through a gap between a rotary and a stationary grinding stone. On contact, the bars and grooves on the stones create compression, shearing and rolling friction forces that disintegrate the fibres into their sub-structural components through fibrillation (Abdul Khalil et al. 2014). The stones usually consist of non-porous resins containing metallic oxides or silicon carbide (Lahtinen et al. 2014; Spence et al. 2011). Compared to the other methods, grinder is more robust and it does not clog as easily, which is why it can be used without fibre-shortening pre-treatments (Spence et al. 2011). According to Iwamoto et al. (2007) grinding treatment of pulp fibres requires less passes through the device to obtain CNF than homogenizing: most of the fibres were observed to be nano-sized after five passes, and subsequent passes did not alter the morphology of the fibres significantly.

Assessing the energy consumption of a specific processing method from literature proves to be difficult, as the results of different studies can vary greatly from one to another. This is due to the use of different materials, process parameters and calculation methods, as well as variations in final CNF grades. One parameter with a considerable impact on the energy demand is the number of passes the raw material is forced through the processing system, which can vary from less than five to more than twenty, depending on the procedure and desired results (Spence et al. 2011; Lahtinen et al. 2014; Abdul Khalil et al. 2014). Other major indicators of energy consumption include fibre consistency, mass flow rate and power (Osong et al. 2015). These will be discussed in more detail in chapter 2.3.

Despite the large variation in the process methods and the subsequent results, the energy demands of different processing methods still seem to follow a general trend

well enough to allow a comparison between them. For example, Spence et al. (2011) reported a remarkable reduction in net energy consumption between homogenization and grinding or microfluidization while obtaining CNF of comparable quality.

For homogenization, the reported net energy consumption values typically vary between 20 000- 30 000 kWh/t (Lindström et al. 2014; Spence et al. 2011), although Eriksen et al. (2008) reported values between 12 kWh/kg and 70 kWh/kg. However, they stress that they did not focus on optimizing energy efficiency during processing. For grinding, the same group reported an energy demand of 3-24 kWh/kg, whereas other groups have reported values of 20 kWh/kg with five passes (Taipale et al. 2010) and 5-30 kWh/kg (Wang et al. 2012). For microfluidization, the energy values are similar to those for grinding. For example, Taipale et al. (2010) reported a value of 22 kWh/t with four passes.

In addition with the methods based on homogenization and grinding, several other processing methods, such as extrusion (Lee et al. 2010), nanopulping (Zhu et al. 2012), and furnish refining (Williamson 2015) are continuously under development. Additionally, a number of other mechanical processes to produce CNF have been used in laboratory scale, such as cryocrushing, electrospinning, ball milling and ultrasonification. However, these methods are difficult to scale up into industrial use (Habibi 2014).

2.2.2. Pre-treatments

As explained in the previous chapter, mechanical processing of CNF can be very energy intensive and susceptible to clogging due to the tendency of cellulose fibres to entangle and aggregate, which results from high surface area and large number of reactive hydroxyl groups on the surfaces. Thus the main purpose of pretreating fibrous raw material before mechanical processing into CNF is usually to facilitate the fibrillation and prevent aggregation during the mechanical processing by altering the surface properties of the fibres. Additionally, another purpose might be to alter the properties of the CNF for certain applications or post-processing methods (Habibi 2014).

The pre-treatments can be divided into mechanical, chemical and enzymatic methods. Of chemical methods, one of the most prevalent is (2,2,6,6-Tetramethylpiperidine-1-oxyl)-mediated (or TEMPO-mediated) oxidation of cellulose. The reaction is applied in aqueous conditions using TEMPO as a stable nitroxyl radical in the presence of sodium bromide (NaBr) and sodium hydrochlorite (NaOCl), as shown in figure 4. As de Nooy et al. (1996) first showed, this reaction is highly selective for the hydroxymethyl groups in polysaccharides, oxidizing them into their carboxylic form. Widely researched since its introduction, the method proved to be a green, simple and cost-effective way to alter the surface properties of cellulose fibres.

The use of TEMPO-mediated oxidation as a pre-treatment prior to mechanical processing of CNF was pioneered by Isogai's group (Saito et al. 2006). They showed that the carboxylic form of fibre surface hydroxymethyl groups weakens the strong hydrogen bond networks between the cellulose fibres, which softens their rigid structure and facilitates their individualization, enabling a remarkably more effortless mechanical conversion to CNF while retaining the original morphology. As a result, the energy consumption of mechanical processing is lowered to less than 2000 kWh/t. According to Pöhler et al. (2010), the resulting nanofibrils are more individualized, thinner (3-5 nm) and less branched, and the material is more homogeneous compared with CNF produced by only mechanical approaches.

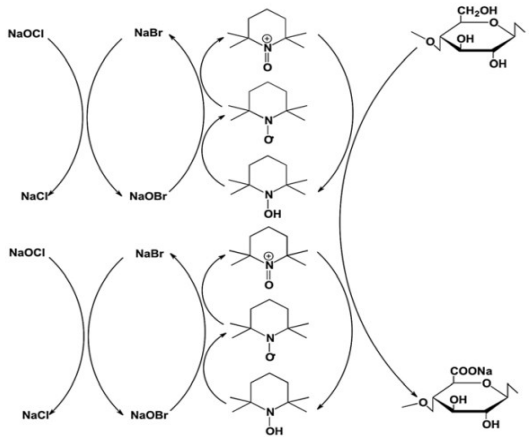

Figure 4. Scheme of the TEMPO-mediated oxidation mechanism of the hydroxymethyl groups of cellulose (Habibi 2014).

Another common chemical pre-treatment that facilitates the fibrillation of CNF is washing to sodium form, i.e. treating the fibres with a sodium bicarbonate ($NaHCO_3$) – solution under acidic conditions to alter the counter-ions on the fibre surface to the sodium form. Scallan and Grignon (1979) were the first ones to report how the nature of counter-ions attached to the charged groups on the fibre surface affect the swelling of the fibres, and to conclude that the sodium form was the most advantageous to the swelling and led to the strongest fibre bonding after refining. Soon thereafter it was found that the swelling of the fibres due to the counter-ion form results in the weakening of their structure and hence facilitates their fibrillation (Lindström & Carlsson 1982).

It has been theorized that the mechanism of the counter-ion –induced swelling is based on the electrostatic repulsion of charged electrolytic gels (Ankerfors 2012; Bäckström, M. and Hammar 2010). According to this theory, the fibre wall can be perceived as a polyelectrolyte gel, whose osmotic pressure and subsequent swelling is dictated by its electrostatic repulsion, which in turn is affected by the electrolyte concentration and pH of the surrounding solution. More precisely, high electrolyte concentration and low pH both lower the electrostatic repulsion of the fibre wall, which in turn reduces the swelling of the fibres due to the decrease in osmotic pressure. The importance of the counter-ions is that they determine the number of free ions in the system, which establishes the electrolyte concentration: a monovalent counter-ion (e.g. sodium), decreases the electrolyte concentration of the solution, maximizing the swelling of the fibre; a divalent counter-ion (e.g. calcium) causes less swelling; and a trivalent counter-ion (e.g. aluminium), serves as a cross-linker and de-swells the fibres (Ankerfors 2012).

Other ways of chemically pretreating cellulose are estherification and etherification. In these processes the fibrillation is facilitated by increasing the anionic charges on the fibre surfaces with the introduction of charged groups. A widely-researched estherification treatment is acetylation, in which acetic anhydrate or acetic acid is used

in the presence of a catalyst such as sulfuric or perichloric acid to acetylate the cellulose chains (Habibi 2014; Isogai 2013).

The most popular etherification pre-treatment is carboxymethylation. Pioneered by Walecka (1956) in papermaking and applied to CNF production by Wågberg et al. (1987), carboxymethylation is an efficient and cost effective way to facilitate CNF preparation. The relatively simple conversion begins by activating fibres with alkali hydroxide, most commonly NaOH, after which indiscriminate hydroxyl groups are converted into carboxymethyl moieties by monochloroacetic acid or its sodium salt. This leaves the fibres highly charged, making them easier to liberate the same authors claimed that the energy consumption of homogenization was reduced from 27 kWh/kg to 0.5 kWh/kg (Wågberg et al. 1987). However, the method has its drawbacks, including the use of the toxic halocarbon reactant (monochloroacetic acid) and the fact that the resulting CNF is even more hydrophilic than before, which can limit the applications involving nonpolar media (Habibi 2014).

Another way to facilitate the mechanical processing of cellulose besides chemical treatments is to utilize the cellulose-degrading enzymes found in nature through biotechnological means. Enzymatic pre-treatment of cellulose is a complex series of processes based on cellulose hydrolysis where different types of enzymatic activities work synergistically to create a cellulase system (Liu et al. 2009). These cellulase systems can be divided into three categories based on their structural properties: endoglucanases, exoglucanases and beta-glucosinades (Percival Zhang et al. 2006).

The use of cellulases in paper and pulp industry have been thoroughly studied (Spiridon & Popa 2000; Viikari et al. 2007), but there are fewer reports concerning CNF production with the method. Pääkko et al. (2007) used a mild endoglucanase treatment prior to microfluidization to produce CNF with diameter in the range of 5-20 nm and good rheological properties. Henriksson et al. (2007) used a similar treatment prior to homogenization to obtain CNF with diameter range of 5-30nm and small DP reduction, resulting in high aspect ratio. Both studies also agree that the enzymatic

pre-treatment facilitates the disintegration of fibres into CNF and removes the issue of clogging.

2.2.3. Post-processing of CNF

CNF can also be further processed after the mechanical treatment to improve their properties or application compatibility. The majority of these post-processing methods are involved with the water chemistry of cellulose fibrils, although they can also be applied to introduce functional groups to the fibrils. The methods can be divided to chemical modifications and nonchemical treatments. The nonchemical treatments mainly consist of thermal and mechanical methods that reduce the amount of water in the CNF, such as filtration, freeze-drying, evaporation, solvent exchange, or use of various additives (Moon et al. 2011).

The chemical modifications are mostly aimed to modify the surface properties of CNF towards a more hydrophobic composition, or to add a range of functional groups to the fibril surface. These modifications can be performed via noncovalent methods such as adsorption of surfactants, oppositely charged entities or polyelectrolytes (Habibi 2014; Xhanari et al. 2011). Another method is to build multilayer CNF films by electrostatic-driven layer-by-layer (LbL) assembly with oppositely charged entities, as demonstrated by Wågberg et al. (2008).

Covalent modifications of CNF can also be performed with a range of methods. There are a number of reports describing a silylation treatment (Gousse et al. 2004), which makes the CNF dispersible in nonpolar solvents, resulting in stable and non-flocculent suspensions. The silane derivatives are also able to stabilize water-in -oil emulsions (Andresen & Stenius 2007), and can be used as an intermediate for further modification (Andresen et al. 2007). A similar way to reduce the hydrophilicity of CNF is urethanization, where a urethane linkage is created between the hydroxyl groups (Siqueira et al. 2010). The surface modification of CNF can also be performed via quickly and reliably linking molecules together in a modular fashion. This is called click-chemistry. For example, Tingaut et al. (2011) have developed a method for modifying CNF films via a series of thiol-ene click reactions. It is also possible to attach polymers

to the CNF surface via a method called grafting (Habibi 2014). It includes two main approaches: “grafting onto” and “grafting from. “Grafting onto” consists of mixing the CNF with an existing polymer and a coupling agent (Benkaddour et al. 2013), whereas in “grafting from” CNF is mixed with a monomer and an initialization agent to induce polymerization from the fibre surface (Lönnberg et al. 2011). One of the main goals of grafting is again to reduce the hydrophilicity of CNF, but the polymer chains can also be utilized as binding sites, or to form polymer matrixes (Habibi 2014).

2.3. Process parameters of CNF production

Like any technical process, the production of CNF has a number of parameters that heavily alter the process conditions, which need to be systematically addressed in order to optimize and standardize the production process. In CNF production these parameters include the settings of processing equipment, and the composition of raw materials and process medium, as well as the process temperature. Additionally, one heavily influential process parameter in mechanical CNF production is simply the number of passes the raw material is fed through the processing equipment.

The settings on the CNF production equipment can be used to affect the nature and intensity of the mechanical forces applied on the fibres. In methods based on homogenizing, the key settings are the operating pressure and flow velocity, as well as the shape and size of the pressure chamber. In friction grinding, the most important settings include the shape and material of the grinding stones, the clearance between the stones and the spinning velocity of the grinding unit (Spence et al. 2011). Additionally, the pressure and velocity of the feedstock stream is also a relevant parameter if the grinding process allows forced feed instead of gravitational feed.

2.3.1. Raw materials

A variety of raw materials can be used to produce cellulose nanofibrils, although wood-based materials, such as solid wood and different types of pulps, are most commonly used (Klemm et al. 2011). Other studied raw materials include agricultural

crops and their secondary products, sugar beet, bagasse, sisal and hemp (Alila et al. 2013; Peresin et al. 2014). The choice of raw material can greatly affect the production parameters of CNF, especially the grinding properties and size distribution of the resulting nanofibrils. For example, several studies have shown that a higher concentration of hemicelluloses facilitates the fibrillation of cellulose fibres and reduces the size of the formed fibril aggregates (Iwamoto et al. 2007; Lahtinen et al. 2014). Similarly, pulps containing lignin are also noted to be more easily fibrillated than bleached pulp (Spence, Venditti, Habibi, et al. 2010).

Additionally, Lahtinen at al. (2014) suggested that due to presence of lignin and hemicelluloses, the refining of unbleached pulp produced finer and more homogeneous CNF than that made from bleached pulp. Spence et al. (2010) also noted that the contents of lignin, hemicelluloses and pectin may affect other properties of CNF, such as sorption and barriers properties as well.

Several studies have established that the correlation between hemicellulose and lignin content and fibrillation efficiency is related to the increase in charge density created by these components, which in turn alters the electrostatic repulsion of the system (Bäckström, M. and Hammar 2010; Fall et al. 2014). As stated in the chapter 2.2.2, it has been known for some time in pulp and paper industry that there is a connection between electrostatic repulsion and fibre swelling (Lindström & Carlsson 1982; Scallan & Grignon 1979). The swelling is believed to result from the increase in osmotic pressure in the fibres that causes more water to flow into the cell wall, which is influenced by the electrostatic repulsion forces (Bäckström, M. and Hammar 2010).

According to Lindström and Carlsson (1982), the requirement for fibre swelling is a sufficient amount of charged groups and sufficient elasticity. They also noted that the charges of the charged groups in the fibres are pH –dependent, and their responses to different pH levels can vary depending on the raw material. Furthermore, as also discussed in chapter 2.2.2, Scalland and Grignon (1979) found that the cationic form of the counter-ions also affects the electrostatic repulsion of the fibres. They concluded

that the sodium counter-ion form creates the greatest number of free ions that contribute to the electrostatic repulsion and thus provides the greatest swelling effect.

2.3.2. Process medium

Although most polar solvents can be used in CNF production, the standard processing medium for CNF production is water (Turbak et al. 1985), and fibre-water –interactions have been studied extensively (Fernandes Diniz et al. 2004; Klemm et al. 2011). However, no studies have been reported, to the author's knowledge, in which the relationships between the ionic composition (purity) of the water and the fibrillation efficiency or product properties have been systematically investigated. In this thesis these relations are examined using regular tap water and reverse-osmosis water (ROV).

Additionally, as mentioned in the previous chapters, the pH of the process medium affects the swelling properties and subsequent fibrillation of the fibres. The mechanism behind this process is that pH affects the deprotonation of the hydroxyl groups in the fibre surfaces, thus altering the charge density and electrostatic repulsion of the system, which in turn alters the osmotic pressure of the fibres that controls their swelling (Grignon & Scallan 1980). The optimal pH for fibre fibrillation is around neutral, where the fibre surface is weakly anionic (Lindström & Carlsson 1982).

Recently, CNF –based composites have gained increasing attention, and as water can be a hindrance in such systems, there have been multiple studies concerning fibrillation in non-aqueous conditions. For example, Shimizu et al. 2010) have developed a method for cellulose microfibrillation in a resin/organic solvent –mixture to form thermoplastic of cured composites. Similarly, Yamazaki et al. (2013) and Takizawa et al. (2014) have both proposed a method for cellulose nanofibrillation in a resin to form a masterbatch without additional solvents.

Besides composites, there are other fibre systems and end applications where a non-water medium can be beneficial. These include for example painting, cosmetics and foodstuff industry, where in many cases water is actively removed after fibrillation, as described in chapter 2.2.3. In addition, it has been found that the use of non-water

solvents and additives in the processing medium can affect the fibrillation properties of CNF and the characteristics of the end product (Carrillo et al. 2014; Lin et al. 2013; Sirviö et al. 2015). Although far less extensively researched, these recent findings could open novel ways to improve the production processes of CNF-based applications by facilitating CNF dispersion or enhancing compatibility with applications. For example, Graveson (2013) described a low-energy method for non-derivatized CNF production using a combination of cyclic organic solvents, such as morpholine and piperidine, and organic or inorganic swelling agents. Paltakari et al. (2012) in turn reported a method where carboxymethyl cellulose (CMC) was used as an additive to improve the quality and reduce the energy consumption of fibrillation. Carrillo et al. (2014) proposed the use of microemulsions based on urea and ethylenediamide as a novel method to facilitate the fibrillation in CNF production with microfibrillation. Aditionally, in his master's thesis, Zheng (2014) studied the effect of polyacrylic acid (PAA) addition on cellulose fibrillation, and concluded that it showed potential as a swelling agent, thus facilitating the disintegration of pulp during refining.

Glycerol, sorbitol and ethylene glycol are interesting additives that appear in several publications. Lee et al. (2010) tested the effects of additives with cellulose affinity, namely ethylene glycol, glycerol and dimethyl sulfoxide (DMSO), on the efficiency of CNF fibrillation. They concluded that all of the compounds managed to accelerate fibrillation by disrupting the hydrogen bond network of the fibrils, but ethylene glycol was the most effective. Both Rouilly et al. (2009) and Hansen et al. (2012) noted changes in the properties of CNF-based films fibrillated with different plasticizers or cross-linkers, including glycerol, sorbitol and ethylene glycol or its derivatives.

Sirviö et al. (2015) very recently reported that using the easily accessible and nontoxic deep eutectic solvents (DESs) as a pre-treatment media for CNF processing can enhance the fibrillation of cellulose as well. The process is still currently unknown, but the group theorize that the solvent can penetrate the fibres and loosen their structure, allowing more efficient fibrillation. They also propose a possibility that a small number of hydroxyl groups are converted to carbamates, which leads, to an extent, to a similar

distortion of the hydrogen bonding network as TEMPO-mediated oxidation or carboxymethylation.

2.4. Properties and characterization of cellulose nanofibrils

As stated earlier, cellulose nanofibrils have a number of so-called nano-specific properties that differentiate them from traditional cellulosic material. These properties include their small size with a diameter ranging from three to a few hundred nanometers (Habibi 2014), high aspect ratio of 100-150 (Siró & Plackett 2010) and large specific surface of 100-200 m^2/g (Lavoine et al. 2012) as well as their tendency to form thin films when dried (Taniguchi & Okamura 1998). However, unambiguous characterization of CNF is challenging due to their heterogeneous nature and considerable variance between different raw materials, pre-treatments and processing methods. For example, the Young's modulus of CNF can vary between 13 and 180 GPa depending on these properties (Josefsson et al. 2013). As CNF contain fibres, fibrils and fibril aggregates with variable dimensions and high degree of branching, their thorough characterization cannot be implemented by a single method. Instead, a combination of methods that operate on several dimensional scales is required (Kangas et al. 2014).

Kangas et al. (2014) reviewed a number of characterization methods and conclude that the best combination of methods to assess the basic properties of CNF includes microscopic evaluation of appearance, morphology and size of CNF fibrils, apparent viscosity measurement as a fast method for assessing rheological properties and transmittance measurement for particle size distribution. They add that visual analysis via light and electron microscopy continues to be the primary characterization method that should always be included in CNF evaluation, despite its drawbacks as being time-consuming and based on subjective assessment of small areas from a large sample. Habibi (2014) agrees on his review that the most important characteristics of CNF are its dimensions, the distribution of dimensions and the rheology of the resulting dispersion.

In addition to the ones mentioned earlier, CNF exhibits a number of other characteristics that are interesting for specific applications. For example the surface properties of chemically modified CNF are important for composite applications, mechanical properties for CNF films or CNF-enhanced paper or packaging applications, and dispersion stability and rheological properties for functional additives (Kangas 2014). Table 1 provides a comprehensive list of the most important properties of CNF and their characterization methods.

Table 1. The most important properties of cellulose nanofibrils and their characterization methods. Modelled after Kangas et al. (2014).

Property	**Characterization method**
Amount of nanomaterial	Fractionation methods (Tanaka et al. 2012)
Particle size and size distribution	Microscopy (light, SEM, TEM, AFM) (Kangas et al. 2014) Transmittance (Saito et al. 2006)
Fibril morphology	Electron microscopy (SEM, TEM, AFM) (Kangas et al. 2014)
Crystallinity	X-ray diffraction (Iwamoto et al. 2007)
Degree of polymerization	Viscosity method (Iwamoto et al. 2007)
Specific surface area	Brunauer-Emmett-Teller (BET) –method (Sehaqui et al. 2011)
Rheology	Low-shear viscosity (Iotti et al. 2011)
Surface charge and chemistry	Zeta-potential (Eronen et al. 2012) Polyelectrolyte and conductometric titration (Junka et al. 2013) X-ray photoelectron spectroscopy (Johansson et al. 2011)
Mechanical properties	Strength properties of CNF films (Rouilly et al. 2009) Gravimetric water retention analysis (Lahtinen et al. 2014)

2.4.1. Fibril morphology and dimensions

Microscopic methods at different magnifications are the primary tools for studying the appearance, morphology, sizes and shapes of CNF. Optical microscopy (OM) is a straightforward method to obtain a quick overview on the fibrillated material, for example on its appearance and homogeneity, but for more accurate details of the fibril dimensions, methods with higher resolutions, such as scanning electron microscopy (SEM), transmission electron microscopy (TEM) and atomic force microscopy (AFM) are more appropriate (Kangas et al. 2014). Of these, SEM has the lowest resolution and is usually not considered adequate for detailed nanoscale evaluation of the fibrils, although with field emission emitters (FE), SEM can be used nanoscale particles can be analysed to some extent, as Abe et al. (2007) showed by using FE-SEM to measure the fibril width of CNF. However, both TEM and AFM can be used to obtain a clearer picture of true nano-size particles due to their higher resolution. Hence, they are best suited for a comprehensive quantitative analysis of fibre dimensions and morphology. For example, Ankerfors (2012) used TEM for studying carboxymethylated CNF with a diameter range of 5-15nm, and Moon et al. (2014) used AFM to observe the topography of CNF, revealing its morphological characteristics at nano-scale. On the other hand, these methods are more laborious and time-consuming than the simpler methods, especially since the irregular shape and polydisperse nature of CNF demand the use of manual or semi-automated microscopy analyses with a high number of images to create an accurate statistical analysis. Additionally, high-resolution microscopy always suffers from some degree of subjectivity during the sample preparation and the choice of the assessed area (Kangas et al. 2014).

There are also indirect ways to efficiently assess the particle size and size distribution of CNF. Saito et al. (2006) used transmittance measurements with a UV-vis spectrometer alongside TEM to discern the decrease in particle size during the processing of TEMPO—oxidized CNF. They explained that CNF suspension becomes increasingly transparent during the disintegration process at the same solid concentration due to the decrease of light scattering from fibrils thinner than the used

wavelengths. Kangas et al. (2014) also recommend the use of transmission-based methods in their review to complement the results obtained via microscopy. Another possible, yet less frequently used technique for estimating the size distribution of CNF is fractionation. Demonstrated by Tanaka et al. (2012), the method utilized micro and nano filters to divide CNF into different size fractions. Another uses for fractionation methods could be to estimate the amount of nanomaterial in CNF, or as a pre-treatment to facilitate microscopic imaging.

2.4.2. Physical structure

The physical structure of CNF can be described by studying its crystallinity, degree of polymerization (DP) and specific surface area (SSA). Crystallinity and DP can both be used to evaluate the level of physical degradation of the fibre during processing, and can also be used to indirectly estimate the strength properties of the fibre. There are a number of ways to measure crystallinity, including X-ray diffraction (XRD), Raman spectroscopy, infrared spectroscopy and nuclear magnetic resonance (NMR) and the results are dependent on the used method (Kangas et al. 2014). Of these, XRD is the most commonly used, although there have been some inconsistencies with the results achieved by it. For example, the crystallinity of CNF has been shown to both decrease (Iwamoto et al. 2007) and increase (Abe & Yano 2009) during grinding. The DP value of CNF can give an estimation of its chain length and breakages along the fibre direction, and it is generally measured via a viscosity method with copper ethyleneamide (Iwamoto et al. 2007).

One of the unique properties of CNF is its high SSA that results from its small size combined with extensive fibrillation and branching. There are several methods to measure SSA, and the results seem to vary from one to another. One of the most prevalent methods include the Brunauer-Emmet-Teller (BET) method, where N^2 adsorption is measured from CNF aerogels and the SSA calculated from the adsorption curve with the BET method, as demonstrated by Sehaqui et al. (2011). They also note that the drying of the sample is a critical step for obtaining representative results, and that the different drying methods can also directly alter the available surface area.

Spence et al. (2010) reported the use of Congo red adsorption as a method to measure the SSA of CNF in a liquid state. However, they stated that the method may suffer from an artefact in lignin-containing raw materials, as they dye has greater affinity for lignin than cellulose. Leppänen et al. (2010) used small-angle X-ray scattering (SAXS) to analyse the SSA of wet, air-dried and re-immersed CNF, with the conclusion that the SSA of wet or re-wetted CNF is much larger than air-dried CNF.

2.4.3. Rheology

The rheological properties of CNF were first studied by Herrick et al. (1983), who found out about their pseudoplastic (shear-thinning) and gel-forming behaviour. In this paper they reported that measuring the relative viscosity of a 2% CNF suspension could be used to determine its degree of nanofibrillation. However, other rheological experiments are much more recent, as the application potential of CNF has lately become more realistic. Pääkko et al. (2007) confirmed that CNF forms a gel-like suspension at concentration of 0,125-5,9 wt%, and observed very large changes in storage modulus (G') throughout this range from 1,5 Pa in 0,125 wt% to 10^5 Pa in 5,9 wt%, the latter being considerably large. Moreover, they state that the G' of CNF is almost 10 times larger than the loss moduli (G'') regardless of suspension concentration. Iotti et al. (2011) provided an insight on the shear-dependent viscosity behaviour at low and high shear rates, using rotational and capillary rheometers for the shear viscosity measurements. Kangas et al. (2014) also recommends the use of low shear viscosity measurements as a relatively fast and easy way to routinely characterize the quality of CNF.

2.5. Applications of cellulose nanofibrils

As stated before, CNF have a wide variety of potential applications due to their unique set of properties. In their comprehensive review on the market projections of CNF-based products, Shatkin et al. (2014) listed the potential applications for CNF, and identified them as high-volume, low-volume and emerging sector applications, as shown in table 2.

Table 2. Identified applications of cellulose nanofibrils and their categorization. Modified after Shatkin et al. (2014).

High volume applications	**Low volume applications**	**Novel and emerging applications**
Automotive	Wallboard facing	Reinforcement fibre
Cement	Insulation	Filtration and purification
Paper coatings	Aerospace	Rheology modifiers
Paper filler	Aerogels	Cosmetics
Plastic replacement	Paints	Medical applications
Hygiene products		Flexible electronics
Textiles for clothing		3D printing

2.5.1. Reinforcing lightweight materials

CNF can be utilized as a dry- and wet-reinforcing agent in paper and packaging applications, due to its ability to enhance the bonding of wood fibril networks (Hentze 2010). Kajanto and Kosonen (2012) reported that the addition of CNF improves the tensile strength of paper even with a reduction in basis weight, which results in a reduction in overall costs. It also enables the use of higher amounts of fines in the paper, which improves its optical properties. Additionally, the addition of CNF can also enhance the barrier properties of paper or board products (Bardet & Bras 2014).

Because of their strength properties, small size and chemical functionality, CNF can also be used as the reinforcing element in polymer composite applications with both hydrophilic and hydrophobic matrixes; although some surface modification is usually needed in order to reduce its affinity for water, which is unwanted in hydrophobic matrixes. CNF composites have been under intensive research during the last decade (Abdul Khalil et al. 2012; Eichhorn et al. 2010; Siró & Plackett 2010) with a wide variety of matrix components. Hydrophilic composites have been composed from such materials as acrylic, epoxy, latex, polyvinyl alcohol (PVOH) and polyurethane resins, as

well as a number of natural polymers including starch, amylopectin and chitosan. Hydrophobic matrixes include polyethylene (PE), polypropylene (PP) and polylactic acid (PLA). With the addition of CNF, it is possible to create strong biocomposites with a remarkable reduction in thickness, leading to savings in material costs. These composites can be used to replace plastic-based materials across the field, including automotive, electronics and aerospace industry. It is also possible to create transparent and biodegradable films that can be utilized in packaging, surfacing or polarizing components such as TV screens or sunglasses.

2.5.2. Rheology modifiers

Due to its rheological properties and non-toxicity, CNF can be used as a rheological agent to control the consistency of a range of emulsions and dispersions, for example in paper, paint, foodstuff, cosmetics and pharmaceutical industry (Turbak et al. 1985). For example, Cavaille et al. (2000) investigated the use of CNF as a thickener in paints, inks, varnish and water-based adhesives, and Pajari et al. (2012) used it as an additive in paper coating. Kleinschmidt et al. (1988) and Yaginuma et al. (2010) reported the use of CNF as a stabilizer and texture regulator in a variety of drinks, sauces, jams, liquid fillings and animal food, while Mondet (1999) used them as a coating agent in cosmetic products.

2.5.3. Transparent films

As stated earlier, CNF have a tendency to form strong, elastic and dense transparent films, which can be utilized in a number of applications. For example, Tammelin et al. (2012) have patented a reel-to-reel method for preparing multipurpose CNF films. In addition to good strength properties, the films also exhibit good barrier properties against oxygen and grease, making them attractive for packaging materials that preserve its contents from spoiling (Österberg et al. 2013). However, further modification is needed to reduce its permeability for moisture, for example by creating multilayer structures with water-resistant polymers. For example, Vartiainen et al. (2014) created a tri-layer structure from polyethylene terephthalate (PET), CNF and polyethylene (LD-PE) that can be used for packaging dry foodstuff, such as nuts, dried

fruits or spices. Additionally, by modifying the surface properties of CNF, the films can also be made to exhibit different functionalities, such as antimicrobial attributes (Andresen et al. 2007). By modifying CNF to improve its electrical conductivity, the films can be used to enhance thin electrical products, such as flexible displays, solar panels, electronic papers and sensor panels (Okahisa et al. 2009; Siró & Plackett 2010).

2.5.4. Other applications

Another important property of CNF is its ability to form dense fibril networks that are useful in a number of applications. Because of its hydrophilicity and large specific surface, CNF networks can absorb and retain a large amount of water, and also release it in a controlled manner. These characteristics can be utilized in a range of medical (Kolakovic et al. 2012; Orelma et al. 2012), foodstuff (Weibel 2001) and hygiene products (Suzuki & Mori 2003; Takai & Konishi 2004). CNF-based nanopapers can also be used as a membrane for matter separation or nanofiltration (Mautner et al. 2014). Similarly, Korhonen et al. (2011) have constructed hydrophobic aerogels that can be used to collect organic impurities from water. Lastly, CNF can form low-density - high-strength foams (Sehaqui et al. 2010) and other porous structures that can be utilized as insulators (Yang et al. 2005; Wicklein et al. 2015), packaging materials or air filters (Shatkin et al. 2014).

2.6. Conclusions from the literature review

Cellulose nanofibrils (CNF), a form of cellulosic nanomaterials, have been under intensive research for the last decade. CNF are nano-scale units isolated from plant fibres via mechanical fibrillation, the most common processing mechanisms being homogenization, microfluidization and friction grinding.

CNF has a lot of potential in a variety of applications as a biocompatible, biodegradable and nontoxic component with a unique set of properties, but the major issue of CNF production has traditionally been its high energy consumption. However, the recent development of chemical and enzymatic pre-treatments has alleviated the energy intensity of the process, which has increased the feasibility of CNF-based applications.

The major uses of CNF are as a reinforcing element, rheology modifier and a component for transparent films.

Overall it seems that a major part of recent studies concerning CNF seem to be focused around their characterization, post-processing treatments and applications. However, there is still much room for systematic research aimed at improving the efficiency of the CNF production process and the properties of the end product. This thesis aims to analyse the relationship between the energy consumption and product quality of CNF manufacturing process, focusing on the composition of the process medium.

3. AIMS OF THESIS

The aim of this Master's thesis was to contribute to the process optimization of cellulose fibril production. The experimental work focused on studying how the composition of the process medium affects the energy consumption and the product quality of CNF manufacturing process. This was conducted by comparing the fibrillation of never-dried birch kraft pulp dispersed in either RO-water, tap water, 100% glycerol, or an aqueous solution with a 5% dose of a green additive. Three separate additives were tested: glycerol, a commercial debonder solution (Prosoft) and a choline chloride – glycerol (1:2) deep eutectic solvent. Prior to processing, the pulp was ion-exchanged to the sodium counter-ion form, which is known to produce optimal swelling and fibrillation conditions. Mechanical grinding with a Masuko supermasscolloider friction grinder was used as the fibrillation method, and each sample was processed five times through the grinder.

To assess the quality of the fibrillated materials, a combination of characterization methods chosen form literature were used. The methods and the parameters they represent were: optical and electron microscopy for the morphology and homogeneity of the fibrils; viscosity measurements for degree of fibrillation and strength of the interfibrillar network; water retention measurements for degree of fibrillation and surface properties; transmittance measurements for the size and dispersion stability of

the fibrils; and fractional analysis for the amount of residual fibres. Additionally, the specific net energy consumption of the grinding process was monitored, and the results of the characterization methods are presented as a function of specific net energy consumption to illustrate the relation between energy efficiency and product quality for each sample.

The main hypothesis for the experimental work was that the swelling and subsequent fibrillation of the fibres dispersed in tap water is disrupted by the multivalent cations found in the tap water, resulting in poorer characteristics and energy efficiency compared those dispersed in RO-water. The dispersion in 100% glycerol and the use additives are hypothesized to improve the swelling of the fibres and thus facilitate the fibrillation process.

4. EXPERIMENTAL WORK

4.1. Pulp preparation

Never-dried bleached birch kraft pulp (Botnia Nordic Birch AKI) obtained from Äänekoski was used as a raw material. The pulp was ion-exchanged (washed) to the sodium form before fibrillation. The washing procedure was based on the method described by Swerin et al (1990) with some modifications. The metal ions were removed by adjusting the pH of the pulp to below 3 followed by filtration and washing with deionized water. The pulp was then treated with 0.5 M $NaHCO_3$ – solution and its pH was adjusted to between 8 and 9 with 1m NaOH. Finally, the pulp was washed with deionized water until the conductivity of the filtration was below 20µS/cm. The consistency of the washed pulp was 26.03% (w/w). After washing the pulp was stored in a refrigerator (+8°C).

Five different samples were prepared from the pulp by diluting the pulp to 2.0% (w/w) consistency. The reference sample (ROV) was diluted with reverse osmosis water with no additives, while the tap water sample (TAP) was diluted with tap water with no

additives. The additive samples (BON, GLY and DES) were mixed with a single 5% (w/w) additive prior to dilution to 2.0% (w/w) consistency with reverse osmosis water. The dose was based on unpublished results on composite studies, where 5% of additives produced a positive response on fibre dispersion and fibrillation, and increasing the dose to 10% did not significantly alter the results. The additives used in the experiment were respectively: Prosoft TQ1003EU (Solenis), a cationic oleylimidazoline debonder (BON); glycerol rectapur (GLY); and choline chloride-glycerol (1:2) deep eutectic solvent (DES). The deep eutectic solvent was prepared by mixing one part choline chloride (Sigma) and two parts glycerol (Sigma, rectapur) in an 80°C oil bath for 2.5 hours in a Reactor-ready Radleys –reactor with 250-280 rpm mixing. The additives were mixed with the pulp for 10 minutes with a Kenwood mixer before dilution. The samples, their abbreviations and process conditions are summarized in table 3.

Table 3. The samples used in this thesis, their abbreviations and process conditions. The sample dispersed in RO-water with no additives acted as a control.

Sample	Process medium	Additive (5%)	No. of passes through Masuko
ROV2	RO-water	(none)	2
ROV3	RO-water	(none)	3
ROV5	RO-water	(none)	5
TAP2	tap water	(none)	2
TAP3	tap water	(none)	3
TAP5	tap water	(none)	5
GLY2	RO-water	Glycerol	2
GLY3	RO-water	Glycerol	3
GLY5	RO-water	Glycerol	5
DES2	RO-water	DES	2
DES3	RO-water	DES	3
DES5	RO-water	DES	5
BON2	RO-water	Debonder	2
BON3	RO-water	Debonder	3
BON5	RO-water	Debonder	5

Additionally, a sample dispersed in 100% glycerol (Sigma, rectapur) was prepared, but the viscosity of the suspension caused the system to overheat during grinding, and the sample was discarded. This is discussed further in the next chapter.

4.2. Fibrillation

All samples received the same fibrillation treatment. The 2.0% (w/w) pulp suspension was first dispersed using an Ystral Dispermix disperser at 30Hz for 10 min, after which the pH was adjusted to between 6.5 and 7.5. The suspension was then fed into a MKZA10-15J Supermasscolloider friction grinder (Masuko Sangyo Co), shown in figure 5. Two modified grinding stones were used: a MKE10-46 for a fine and a MKGA10-80 for an ultra-fine particle size. Both stones have a diameter of 10 in, and MKE10-46 is made from silicon carbide and resins, while MKGA10-80 is made from non-porous aluminium oxide and resins. The geometry of the stones creates a dispersing effect during contact grinding, while simultaneously defibrillating the fibres with abrasive and cyclic shear forces. The slurry was passed a total of five times through the grinder using the MKE10-46 stone for the first two passes and the MKGA10-80 for the last three passes. Samples were collected after two, three and five passes through the grinder.

Figure 5. Masuko Sangyo ultrafine friction grinder (MKZA10-15J) equipped with MKE10-46 stones made from aluminium oxide and resins.

The optimal grinding process parameters were adjusted during trial grinding sessions. The clearance between the stones was adjusted by moving the lower stone to a desired distance from the upper stone. In some earlier studies (Suopajärvi et al., 2010, Wang et al., 2012), the clearance value has been chosen as the primary control parameter and indicator of output material quality. However, as Lahtinen et al. (2014) have stated, it was found in the trials that the clearance values do not take the thermal expansion of the stones into account during grinding, as they only measure the distance the lower stone has been moved from a pre-determined zero point of clearance. The operating power of the grinder motor, on the other hand, is always correlative to the actual clearance, and was found a more reliable primary operating parameter in the trials. The operating power was monitored through a frequency converter attached to the grinder.

During the trial runs the operating power levels were optimized for each pass through the grinder. The rotation speed was fixed to 1500 rpm in the first two passes and 1700 rpm for the last three passes. The pH of the samples was adjusted to 6.5-7.5 after the first and last passes. Unfortunately, the MKE10-46 stone was broken between the trials and sample runs and was replaced with a similar stone, which needed whetting to achieve similar performance as the previous stone. However, the whetting of the stone and adjustment of grinding power levels could not be perfectly calibrated due to time concerns, which resulted in un-optimized settings for the first two passes through the grinder. The whetting also caused small pieces of the grinding stone to mix with the samples during fibrillation despite intensive rinsing, which interfered with the transmittance measurements. This is explained further in chapter 5.4.1.

The grinding of the sample dispersed in 100% glycerol was halted during the second pass. The friction caused by the high viscosity of the suspension caused the system to overheat despite liquid cooling. Additionally, the viscosity caused the operating power to reach its maximum even before the clearance between the stones was at the desired levels for fibrillation. At this point, adjusting the clearance did not alter the power level even though the grinding stones came in contact with each other and

burned the fibres between them, which made the operating of the process impossible. Hence, the grinding was discontinued and the samples discarded.

4.3. CNF characterization

4.3.1. Optical microscopy

Fibrillated samples were first dyed with 0.5% Congo red solution (ratio 1:1) by mixing the components with vortex, and then further diluted with reverse osmosis water on the microscope slide (ratio 2:1). Optical microscopy was performed with an Olympus BX 60 microscope equipped with a ColorView12 camera.

4.3.2. Field emission scanning electron microscopy (FE-SEM)

For the scanning electron microscopic imaging, the fibrillated cellulose samples were frozen in a freezer (-25°C for an minimum of 30 min) and dried with a pre-cooled freeze-drier overnight at -60°C and 200mbar. The samples were coated twice with a platinum/palladium (Pt/Pd) -alloy using Agar High Resolution Sputter Coater. The imaging was done with a Zeiss Merlin field emission scanning electron microscope (FE-SEM).

4.3.3. Apparent viscosity

Apparent viscosity of the fibrillated samples was measured with a Brookfield RVDV-III rheometer and a vane spindle. The method was modified after Kangas et al. (2014), which is based on vane geometry as described by Barnes and Nguyen (2001). Vane spindle V-73 was used for the measurements of TAP, BON and DES, and vane spindle V-75 was used for the RO-water control and glycerol-treated sample due to their greater viscosity. The effect of the spindle was taken into account by using yield multiplier constant (YMC) found in the Brookfield operator manual (M13-167-B0614). The YMC was 10 for spindle V-73 and 40 for V-75.

The fibrillated samples were diluted to a 1.5% (w/w) concentration with Milli-Q water and dispersed with an Ultra-Turrax disperser at 8000 rpm for 1 min. Viscosity measurements were performed in a 250ml Pyrex beaker, and each sample was left to

settle for a minimum of 30 min in room temperature after the dispersion. This allowed the samples to regain their initial viscosity. The temperature of the samples was maintained at 20±1°C with water baths.

The measuring program registered a total of 480 measuring points with one-second intervals: the first 300 at vane speed of 0.5 rpm and the remaining at vane speed of 10 rpm. The apparent yield stress was measured from the torque peak of the 0.5 rpm measurements, and the apparent viscosity from the final five of the 10 rpm measuring points. Two parallel measurements were taken from each sample.

4.3.4. Water retention

Water retention of the fibrillated samples was measured using a pressure filtration method (denoted ÅAGWR method), which is described in TAPPI test method T 701 pm-01 and by Sandas et al (1989). Figure 6 shows the design of the measurement apparatus. The method utilizes gravimetric determination of the aqueous phase of the sample penetrating through a filter membrane and absorbed by a blotter paper. For this thesis, the method was modified as described by Lahtinen et al (2014) to make it more suitable as an on-site routine measurement for fibrillated samples with short pressure filtration and good reproducibility. According to these modifications, the water retention value was represents the ratio of the mass of water retained in the sample after 30 seconds under a pressure of 0.5 bar compared to its oved dry mass.

The fibrillated samples were first diluted to 0.2% (w/w) concentration with Milli-Q water and sonicated with a Branson digital sonifier 450 (400W, Emerson Electric Co) with a 102C tip for two minutes with 25% amplitude. The temperature of the samples was fixed to 21°C. Ten pieces of 5cm x 5cm absorbing blotter papers (Whatman International Ltd., Schleicher & Schuell Chromatography Paper, 17 CHR, no. 3017-8355) were weighed and placed on the bottom plate. The membrane filter and the sample cylinder were placed on top of the papers. The membrane filter is a non-hygroscopic polycarbonate filter with a 5.0-µm mean pore size (GE Water & Process technologies, material no. 1215632).

The system was then sealed between the sample cylinder and bottom plate with pressurized air, and a sample of 3 ml was poured into the test cell and the plug was closed. The test cell was then pressurized for a 30 second period, after which the blotting papers were re-weighed to determine the amount of liquid de-watered from the sample. Three parallel measurements were conducted for each sample.

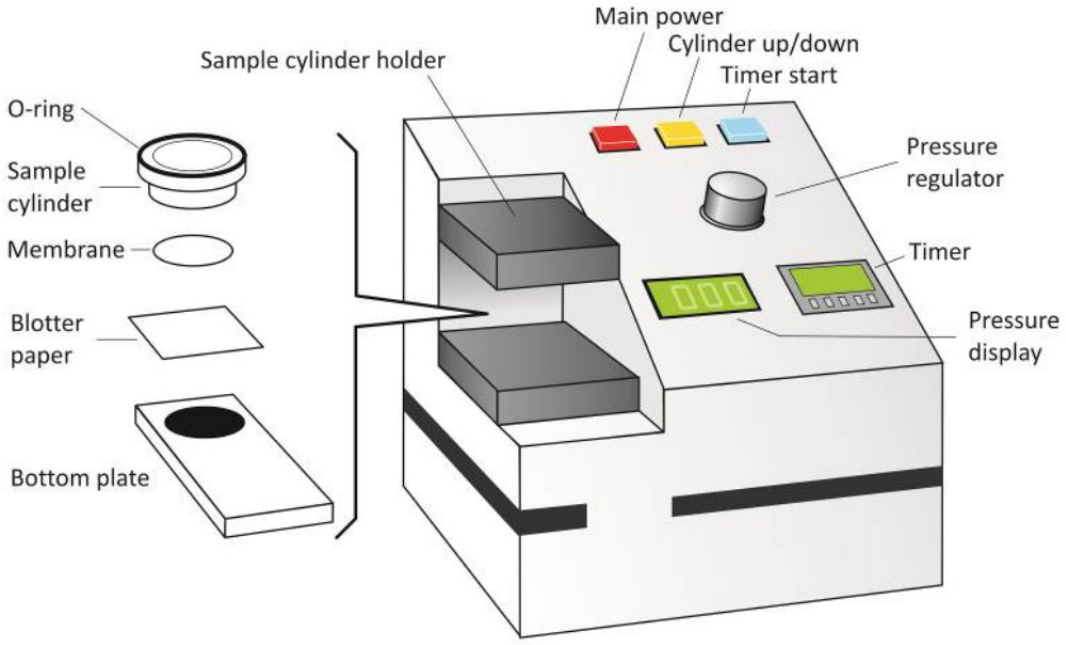

Figure 6. A schematic of gravimetric water retention analysis apparatus (Lahtinen et al. 2014).

4.3.5. Transmittance measurements

Transmittance was measured with Perkin Lambda 900 UV-VIS spectrophotometer with the protocol used by Kangas et al (2014). The samples were dispersed to 0,1% concentration with Milli-Q water, dispersed similarly as in viscosity measurements with an Ultra-Turrax dispenser and sonicated similarly as in water retention measurements. The samples were analysed within one hour of the dispersion in order to prevent flocculation and sedimentation. The transmittance was measured at wavelengths between 200 and 800 nm.

A transmission measurement combined with a settling/sedimentation rate measurement was performed using a TurbiScan LAB Expert (Formulaction) apparatus,

which measures the specific height of sedimentation at a given time frequency with both transmittance and backscatter detectors. Each sample was diluted to 0,1% (w/w) concentration and dispersed with Ultra-Turrax disperser at 8000 rpm for 1 min prior to measurements. The measurements were performed every 5 minutes for 2 hours. The change of height of the sediment during the time interval (ΔH) was calculated for each sample using the TurbiScan software.

4.3.6. Residual fibres

The amount of residual fibres were measured with the FibreLab™ analyser (Metso Oyj), modified after the method described by Chinga-Carrasco (2013). The device analyses fibre flow through a narrow capillary at low consistency. A laser light source within the capillary is used to control two CCD cameras that capture images of the fibres. These images are then processed by FibreLab software to provide several measurements from the fibres, such as fibre length, width and average fines content. The camera measuring fibre length has a resolution of 10µm, and as such does not detect CNF, which is utilized in this experiment to detect the amount of unfibrillated residual fibres in each fibrillated sample.

The measurements were performed in accordance with the FibreLab™ owner's manual (KO2642V1.0EN). The fibrillated samples were diluted to 0.002% (w/w) concentration with tap water and mixed for 10 minutes with a laboratory mixer. Then a 50 ml sample (2 mg of fibre) was fed through the FibreLab analyser.

5. RESULTS AND DISCUSSION

In this study, the differences between producing CNF immersed in tap water and RO-water and the effect of three environmentally sound additives were studied by producing and characterizing CNF samples. The processing of the samples was conducted with a Masuko friction grinder, and the results of the characterization methods are presented as a function of specific net energy consumption of the

grinding process to illustrate the relation of quality and energy demand of the samples. The energy consumption after each pass through the grinder is shown in table 4.

Table 4. Specific net energy consumption of the samples after two, three and five passes through the Masuko friction grinder, respectively. The unit is kWh/kg. ROV=the control dispersed in RO-water; TAP=sample dispersed in tap water; BON=sample treated with 5% Prosoft debonder; DES=sample treated with 5% choline chloride-glycerol (1:2) deep eutectic solvent; GLY=sample treated with 5% glycerol.

	Passes		
Sample	2	3	5
TAP	2.14	2.49	5.29
ROV	2.54	3.07	5.82
BON	1.49	1.87	4.65
DES	1.72	2.13	4.87
GLY	2.69	2.92	5.21

The fibres dispersed in 100% glycerol are not included in the results and discussion as the grinding process was discontinued and the samples discarded. The reason behind this is that the high viscosity of the suspension caused the system to overheat and rendered the operation of the process impossible during the second pass through the grinder, as explained in section 4.2. However, the high viscosity of the suspension after one pass through the grinder is an interesting, and further studies with different doses of glycerol in the process medium are suggested.

5.1. Morphology

Visual representations of the fibrillated samples after three and five passes through the grinder are presented in fig 7. These images give a good preliminary estimation of the characteristics of the samples. He images after three passes show that the untreated RO-water control (ROV) and the sample treated with 5% glycerol (GLY) appear to hold their form the best, indicating they have the highest levels of viscosity, while the sample treated with 5% Prosoft cationic debonder (BON) appears the least viscous and with the most noticeable water separation. It also has a whiter and less

translucent colour than the other samples. The visible differences between the RO-water control and tap water treated sample are also noteworthy. This observation supports the theory that the divalent cations present in tap water disrupt the swelling of the fibrils by reversing the sodium form of the fibre surface described by Grignon & Scallan, (1956), which in turn leads to less efficient fibrillation of the fibres.

After five passes through the grinder the visual characteristics of the samples are significantly evened out to the point where little differences can be seen. In fact, the viscosity of the RO-water control and glycerol-treated sample seem to have decreased, implying that the point after which further grinding does not improve its properties has been reached at rather low energy levels for these samples. This statement becomes increasingly apparent and is further discussed while analysing the other results.

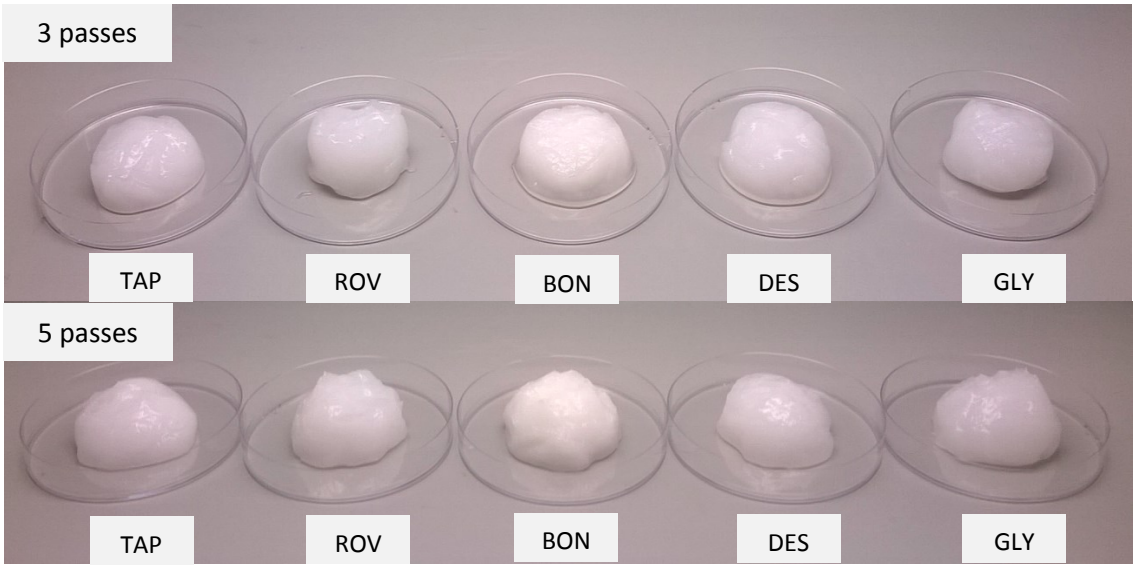

Figure 7. Images of the fibrillated samples after three and five passes through the Masuko grinder, respectively. ROV=the control dispersed in RO-water; TAP=sample dispersed in tap water; BON=sample treated with 5% Prosoft debonder; DES=sample treated with 5% choline chloride-glycerol (1:2) deep eutectic solvent; GLY=sample treated with 5% glycerol.

Figure 8 shows the optical microscope images after two, three and five passes in the Masuko grinder. The images give a good overview on the particle size, morphology and

homogeneity of the samples and enable visual evaluation on their degree of fibrillation and amount of unfibrillated fibres and fibre fragments. The images also complement other characterization methods as the observations on the morphology of the samples help to explain a certain characteristic found with the other characterization methods.

According to the microscopic images, the RO-water control and the sample treated with glycerol seem the most fibrillated after two and three passes, which correlates with the images of the samples shown in figure 7. Their degree of fibrillation and particle morphology also seem fairly similar, which would suggest that the 5% (w/w) addition of glycerol may not have a significant effect on the fibrillation process.

The sample treated with debonder looks to be the least fibrillated after two and three passes. It shows a great number of unfibrillated fibre fragments that are also shorter compared to those in the other samples. However, the degree of fibrillation of the debonder sample seems to greatly increase after five passes. Again, this correlates well with the visual representations. Another noticeable feature of the debonder sample is the great amount of flocks and fibre aggregates shown in the images. One possible explanation for these observations is that the cationic and polymeric debonder acts as a flocculant by attracting the anionic groups (AG) found in the surface of cellulosic fibres (Sjöström, 1989). This effect could also be the cause for the lower degree of fibrillation and shorter fibre fragments that is noticeable in the samples.

The degree of fibrillation and number of unfibrillated fibres of the tap water sample and the sample treated with choline chloride-glycerol (1:2) DES seem to fall somewhere in the middle among the samples. Their appearances are also fairly similar to one another, suggesting that it affects the swelling and subsequent fibrillation of the fibres in a somewhat similar fashion as the divalent ions in tap water.

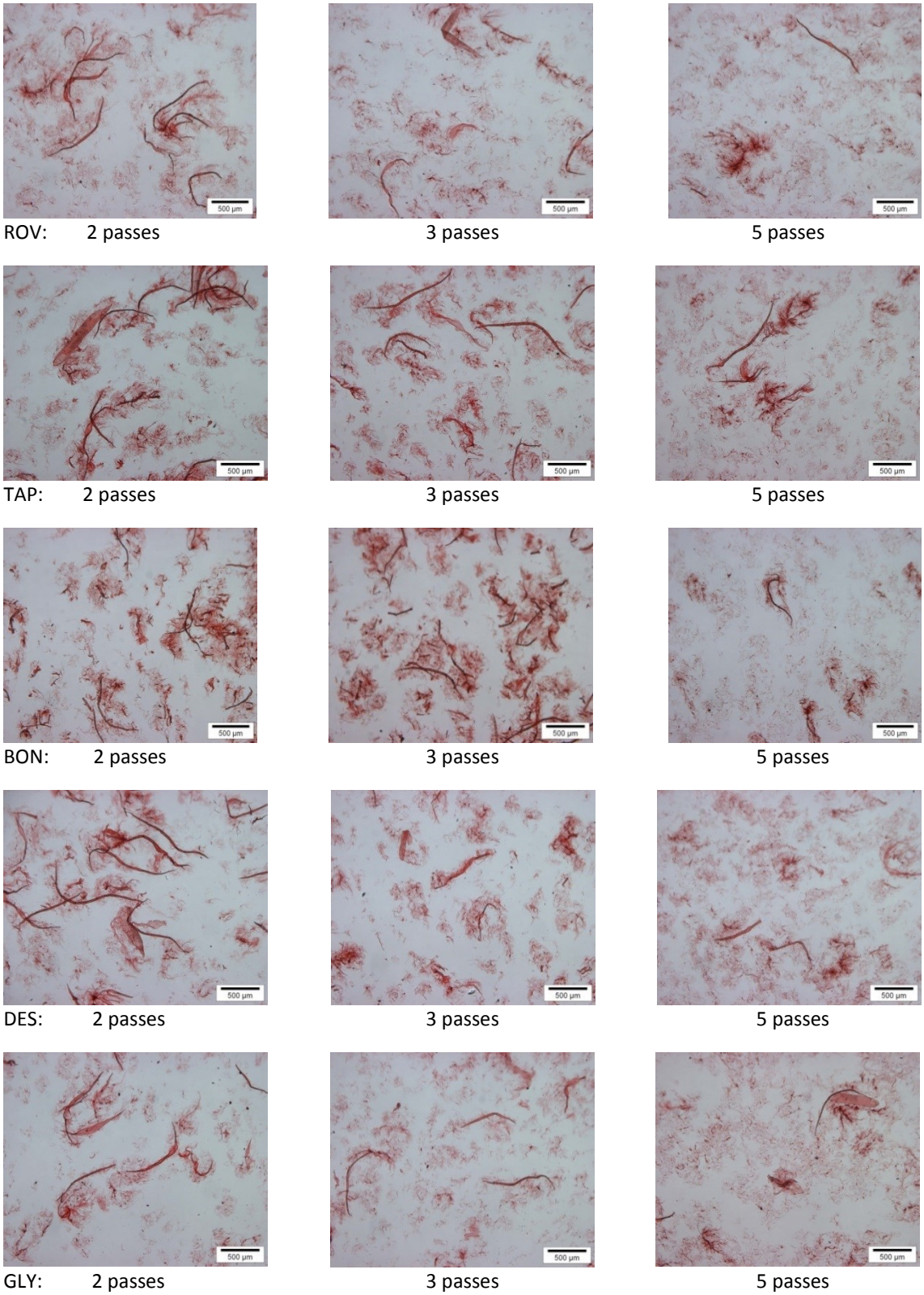

Figure 8. Optical microscopy images of the fibrillated samples after two, three and five passes through the Masuko grinder. ROV=the control dispersed in RO-water; TAP=sample dispersed in tap water; BON=sample treated with 5% Prosoft debonder; DES=sample treated with 5% choline chloride-glycerol (1:2) deep eutectic solvent; GLY=sample treated with 5% glycerol.

The scanning electron microscopy (SEM) images from the samples passed five times through the grinder are shown in Figure 9. SEM images were used to more accurately assess the structural and dimensional appearances of the fibrillated samples. The images showcase the differences in the morphology of the fibres between the samples.

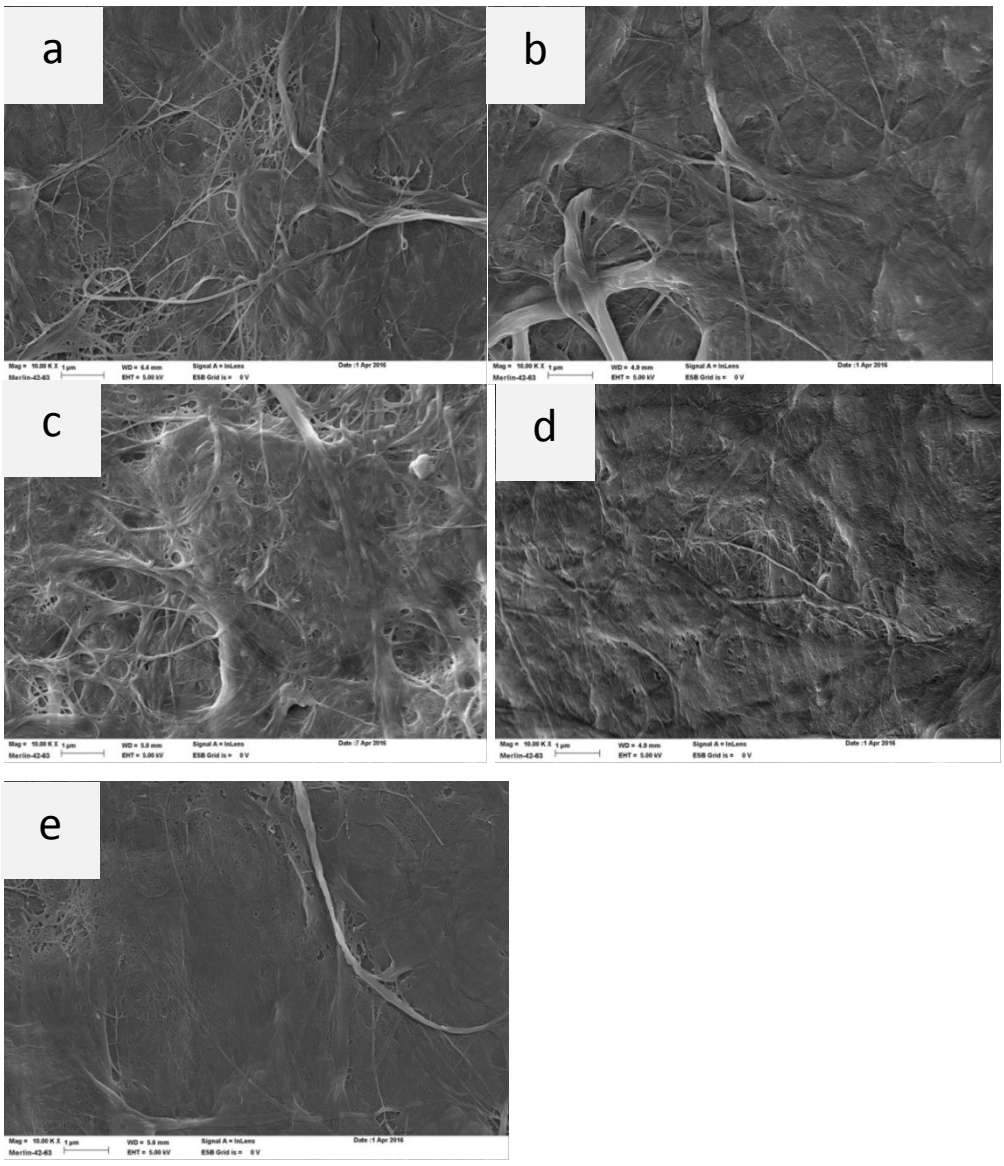

Figure 9. Scanning electron microscope images of the fibrillated samples after five passes through the grinder a) the control dispersed in RO-water, b) sample dispersed in tap water, c) sample treated with 5% Prosoft debonder, d) sample treated with 5% choline chloride-glycerol (1:2) deep eutectic solvent, and e) sample treated with 5% glycerol. Scale bar is 1µm.

The images show that the tap water sample contains rather thick fibres, and the material is fairly heterogeneous. The RO-water control, on the other hand has thin and well-fibrillated fibres, reinforcing the hypothesis that fibres immersed in RO-water swell more and thus fibrillate more efficiently than those immersed in tap water. The fibres in the debonder sample are rather heterogeneous, and bundled in a bulky flock-like structure, further showcasing that the cationic debonder seems to act as a flocculant in the fibre system. All of the samples exhibit the tendency to form layered structures, but in the samples treated with choline chloride-glycerol (1:2) DES and glycerol this tendency seems more pronounced. Especially in the glycerol sample the fibres seem to form a sleek, even layer. The reason behind this phenomenon is unclear, but it could showcase an improved tendency for film formation. It could also be an artefact caused by the presence of glycerol, which may form a smooth mattress between the fibres.

5.2. Rheological properties

Viscosity is a measure used to describe a suspension's internal resistance to gradually deform under shear or tensile stress, i.e. its resistance to flow. In fibril suspensions, an increase in viscosity generally implies a greater degree of fibrillation. The reason behind this phenomenon is that fibrillation of celluloses increases the number of fibre particles and their branching, which in turn increase the number of fibril-fibril interactions and lead to more internal friction within the suspension. Viscosity measurements can therefore be used to verify the degree of fibrillation of fibrillated material.

However, the viscosity of fibrillated celluloses is also known to be dependent of the aspect ratio of the fibrils. Fibrillated fibrils with high branching and aspect ratio are able to form strong interfibrillar networks that lead to high viscosity, and although prolonged fibrillation increases the branching of the fibrils it also shortens them, and the decrease in aspect ratio of the fibrils eventually leads to the weakening of the fibril network and consequent lowering of viscosity. Hence, the viscosity of fibrillated

materials typically peaks at a certain degree of fibrillation and starts to decrease with further processing.

In this work, the rheological properties of the fibrillated samples were measured with a low shear viscosity measurement using a spindle based on vane geometry. According to Lahtinen et al, (2014), the method is widely accepted as a convenient way to test viscous, polydisperse materials and particularly advantageous with heterogeneous materials such as fibrillated celluloses. The results from the viscosity measurements are shown in figure 10. As seen from the images, the yield value and apparent viscosity at 10 rpm behave very similarly to one another, and are referred simply as 'viscosity' values hereon. It is also noticeable that the results are in line with the observations made from microscopic imaging.

All of the fibrillated samples in this study except for the sample treated with debonder seem to exhibit the viscosity peaking behaviour explained before at grinding energy levels between 2 and 3 kWh/kg. However, due to the lack of measurements from the first pass through the grinder, the exact energy level of the peak viscosity for the RO-water control, tap water sample and the sample treated with glycerol remain unknown as their viscosity is already decreasing after two passes.

The viscosities of the RO-water control and the sample treated with glycerol are much larger than those of the other samples after two passes, but decrease heavily with further grinding. This behaviour suggests that these samples exhibit a significant degree of fibrillation already at grinding energy levels below 3 kWh/kg, and that the aspect ratio of the fibrils begins to decrease after this, resulting in a loss of viscosity. This might indicate that grinding with the finer MKGA10-80 stones after three passes was too intensive for these samples. It is also notable that the sample treated with glycerol behaves very similarly to the RO-water control, suggesting again that the 5% (w/w) addition of glycerol has little effect on the fibrillation or rheological behaviour of the sample pulp.

The viscosity of the samples dispersed in tap water and treated with choline chloride-glycerol (1:2) DES is considerably lower than that of RO-water control throughout the

process, and especially after two and three passes through the grinder. This implies that, contrary to the hypothesis, the choline chloride in the DES loses its complex form in aqueous solutions and becomes a halide salt that disrupts the fibrillation similarly as the divalent cations in tap water. Their viscosity also does not drop dramatically after the peak viscosity is reached as happens with the RO-water control and glycerol sample. A possible explanation for this behaviour is that because the tap water and DES-treated samples are less fibrillated and more heterogeneous than RO-water control after two and three passes, the benefits of further fibrillating their long residual fibres for five passes even out the disadvantages of reducing the aspect ratio of the already fibrillated fibrils, leaving the net viscosity closer to a state of dynamic balance.

The viscosity of the debonder-treated sample is significantly lower compared to the other samples after two and three passes, suggesting again that the cationic and polymeric debonder heavily disrupts the fibrillation of the pulp or the formation of the interfibrillar network. A possible mechanism for this is that the debonder creates fibre flocks that are cut to pieces instead of fibrillating, leading to heterogeneous material with generally shorter aspect ratio. The major increase of the debonder sample at higher grinding energy inputs indicates that the degree of fibrillation greatly increases after intensive processing with the finer grinding stones. It also seems that the sample was the only one not reaching its peak viscosity after five passes through the grinder, suggesting that further grinding could still improve its properties.

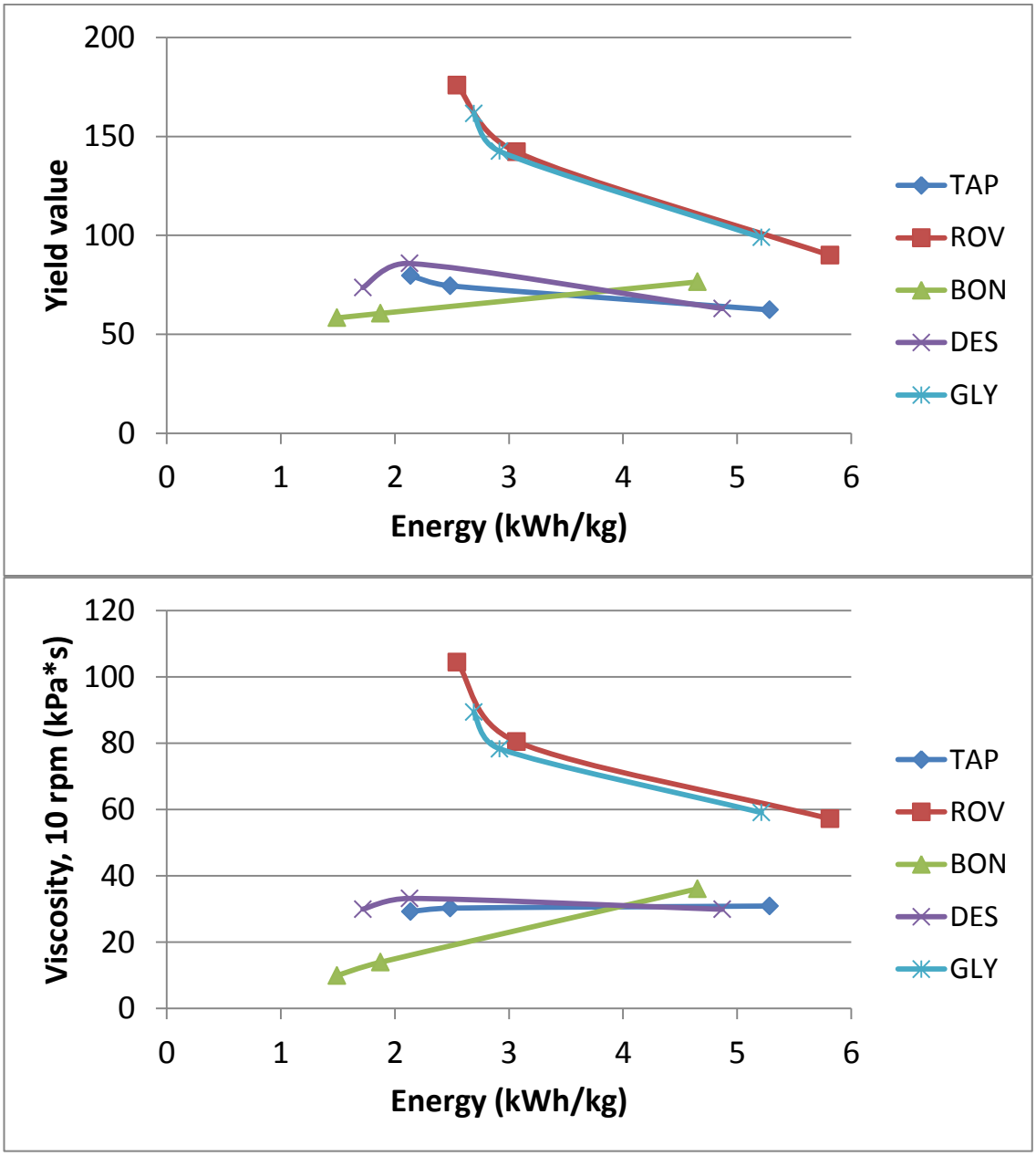

Figure 10. Yield values and low-shear viscosities of fibrillated cellulose samples. ROV=the control dispersed in RO-water; TAP=sample dispersed in tap water; BON=sample treated with 5% Prosoft debonder; DES=sample treated with 5% choline chloride-glycerol (1:2) deep eutectic solvent; GLY=sample treated with 5% glycerol.

5.3. Gravimetric water retention capacity

Gravimetric water retention (GWR) capacity of fibrillated celluloses measures the capacity of CNF to hold water under pressure filtration. In the measurement, free water not bound in the hydroxyl groups of the CNF is removed from the fibre mat

through a semipermeable membrane. As fibres fibrillate during friction grinding, the amount of open fibril surfaces with available hydroxyl groups increases, resulting in improved water retention capacity. Therefore GWR can be used to indirectly measure the degree of fibrillation of the fibres. Additionally, alterations in the hydrophilicity and surface properties of the fibrils caused by pre-treatments or additives can also be detected with the method.

The results from the GWR method (also called ÅAGWR method) are shown in figure 11. Again, the results seem consistent with the other measurements. The RO-water control and sample treated with glycerol exhibit the greatest GWR values that peak after three passes through the grinder, confirming that these samples exhibit a high degree of fibrillation between grinding energy levels of 2 and 3 kWh/kg and that further grinding does not seem to improve the fibrillation of these samples. Similarly to previous observations, the sample treated with glycerol behaves very similarly as the RO-water control. It seems clear that the effect of glycerol on the fibre fibrillation is either very similar to RO-water or small enough to be overshadowed by the significant swelling of the fibres caused by RO-water alone.

The samples dispersed in tap water and treated with choline chloride-glycerol (1:2) DES both have low GWR values after two passes but begin to significantly increase at three and five passes through the grinder. They do not seem to exhibit a clear peaking behaviour, but the increase in GWR becomes less pronounced after the same energy levels between 2 and 3 kWh/kg as with the RO-water control and glycerol-treated sample. The increase of the GWR of the tap water sample is specifically dramatic between two and three passes, while the increase of the DES-treated sample is overall much less pronounced and does not reach the same level. Combined with the observations from microscopic imaging, these results indicate that the addition of the choline chloride in the DES might alter the surface properties of the fibres, although the mechanism for this is unclear.

In accordance with the previous results, the sample treated with the debonder exhibits the lowest GWR capacity of the samples throughout the fibrillation process. However,

the GWR values of the debonder sample are especially low compared to the results of the previous tests. They approach zero after two and three passes, and while improving considerably after five passes still remain significantly lower compared to the other samples at all energy levels. These results suggest that the debonder not only disrupts the fibrillation of the fibres, but might also alter their surface properties. A possible explanation is that the cationic polymers attach to the hydroxyl groups of the fibres, reducing their interactions with water. Overall, while the fibrils treated with the debonder seem to fibrillate poorly compared to untreated fibres, they might have potential in applications where low viscosity and easy water removal are desired.

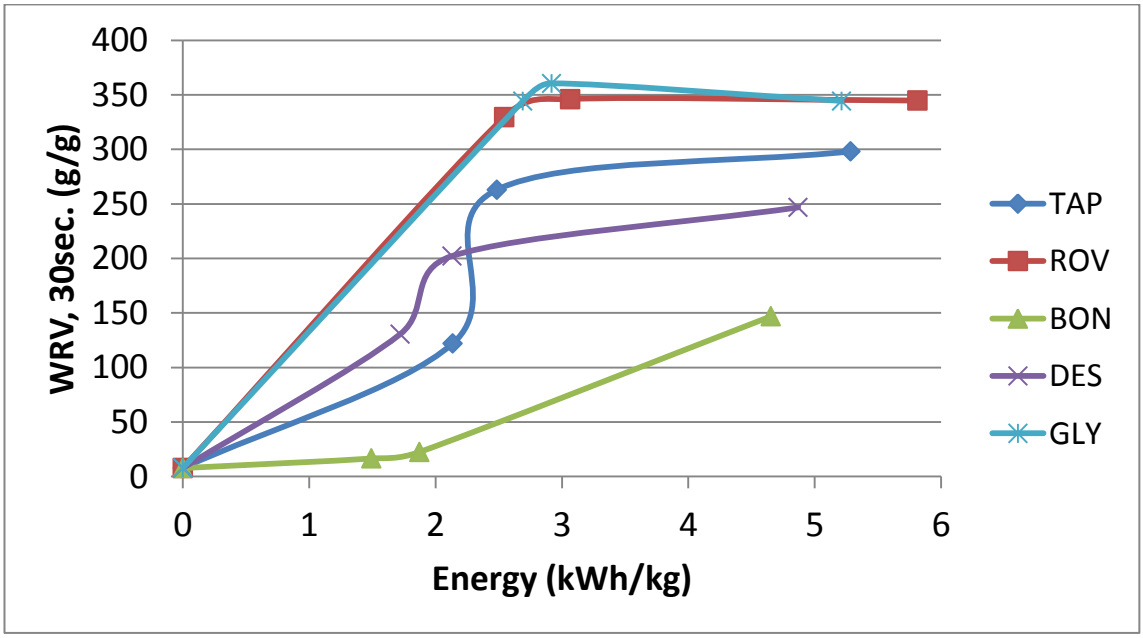

Figure 11. Gravimetric water retention values of the fibrillated samples. ROV=the control dispersed in RO-water; TAP=sample dispersed in tap water; BON=sample treated with 5% Prosoft debonder; DES=sample treated with 5% choline chloride-glycerol (1:2) deep eutectic solvent; GLY=sample treated with 5% glycerol.

5.4. Transmittance measurements

5.4.1. UV-VIS transmittance measurements

Light transmittance is a measure that can be used to determine the particle size of CNF suspensions, although it can also be affected by particle shape and colour, and the differences in refractive indexes of the particle and the sample fluids. As explained in the literature review, finer materials tend to generally have higher transmittance than coarse materials, although the measure is known to be sensitive toward larger particles in the sample (Kangas et al, 2014).

In this work, the transmittance measurements were carried out as described in the materials and methods. However, due to the breaking of the first MKE10-46 grinding stone and the subsequent whetting of the replaced stone explained in chapter 4.2, the fibrillated samples contained some amounts of dark particles chafed from the stone surface. These particles heavily interfered with the transmittance measurements, rendering the results unpublishable.

5.4.2. TurbiScan settling measurements

Transmittance measurements were also carried out with TurbiScan Lab Expert Apparatus to estimate the sedimentation behaviour, or dispersion stability, of the samples. The dispersion stability of a fibril suspension often correlates with the specific surface area and aspect ratio of the fibrils, although it can also be affected by the use of additives. This means that similarly to viscosity and water retention measurements, it can be used to gain information on the optimal level of processing where the degree of fibrillation is high but the aspect ratio has not begun to significantly decrease. Moreover, high dispersion stability is a desired quality in emulsion applications.

These measurements, shown in figure 12, were seemingly unaffected by the artefacts caused by the particles chafed from the grinding stone as the particles sediment with the fibril suspension. ΔH measures the change of height of the sediment at any given time compared to the original level, meaning that the larger the value, the more the

suspension has sedimented. Hence, the smaller ΔH value a fibril suspension has the better its dispersion stability is. In figure 12, the peak value of ΔH after two hours of settling time is presented for each sample as a function of grinding energy. This way of presentation gives an overview of the dispersion stability for each sample. More detailed presentations that show the sedimentation process for each sample as a function of time are found in appendix.

The results from the sedimentation measurements show that the dispersion stability of RO-water control and the sample treated with glycerol are the highest after two and three passes through the grinder. In fact, their ΔH is zero at these points, meaning that they remained completely stabile during the measurement period of two hours. However, the stability of RO-water control greatly decreases after five passes through the grinder, suggesting that the aspect ratio has begun to dramatically drop during prolonged grinding. On the other hand, the stability of the sample treated with glycerol remains very high after five passes, which might indicate that the addition of glycerol increases the stability of the fibril suspension even when the aspect ratio of the fibrils has decreased.

The dispersion stability of the tap water sample begins with low stability after two passes through the grinder, but rapidly increases after three passes and the ΔH reaches zero after five passes. The sample treated with choline chloride-glycerol (1:2) DES begins at relatively high level of stability after two passes and alters very little with further energy input. This would suggest that either the choline chloride ions affect the settling behaviour of the suspension through electrostatic forces, or that the glycerol from the DES improves the dispersion stability of the fibril suspension, as implied by the results from the sample treated with glycerol (GLY).

The debonder sample has a unique settling behaviour, as it begins at a very low stability after two passes, then its stability dramatically increases after three passes but decreases again after five passes. Additionally, as seen in the data in the appendix, the sample BON5 has an area with high back scatter at the middle of the sample, not at the top as in the other samples. This might indicate that the settling of the

suspension does not occur through gravitational sedimentation, but instead by forming stable cloud-like flocks in the suspension, probably around the cationic polymers of the debonder.

It is also worth highlighting that all of the samples exhibit a high level of dispersion stability between the energy levels 2 and 3 kWh/kg, or after two or three passes through the grinder depending on the sample. Based on this and the other measurements, this seems to be the 'optimal' level of grinding energy, where the fibrils presumably exhibit high level of fibrillation and the aspect ratio has not yet began to drop significantly, leading to a strong interfibrillar network.

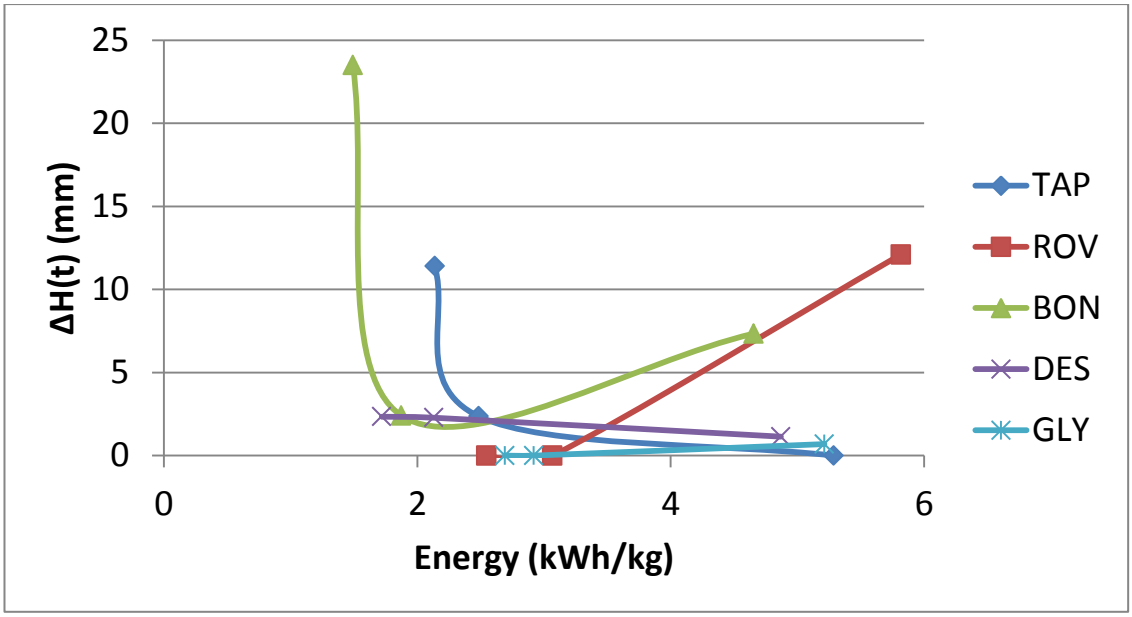

Figure 12. The sedimentation levels of the fibrillated sample suspensions measured with TurbiScan. ROV=the control dispersed in RO-water; TAP=sample dispersed in tap water; BON=sample treated with 5% Prosoft debonder; DES=sample treated with 5% choline chloride-glycerol (1:2) deep eutectic solvent; GLY=sample treated with 5% glycerol.

5.5. Residual fibres

The amount of residual fibres in the fibrillated samples was measured using the Fibrelab™ analyser. As explained in the materials and methods section, the minimum resolution of the analyser is 10 µm, and the average length of a nanofibril is well below

that, meaning that only unfibrillated fibres and fibre fragments will be detected. During the grinding process, the amount of detected fibres usually increases at first due to the cutting of the long fibres, but begins to decrease after prolonged grinding as the fibres disintegrate into shorter fibrils.

The results of the fractional analysis, shown in figure 13, demonstrate that the amount of residual fibres after two and three passes through the grinder decreased with the samples in the order of BON > DES > TAP > ROV > GLY. After five passes, all the samples approach a similar level of residual fibres, and as the results below 5000 pcs/mg are more susceptible to variance, it is not possible to reliably distinguish any significant differences between these points.

Again, the RO-water control and the sample treated with glycerol exhibit very similar behaviour, strengthening the previous notions of the ineffectiveness of the 5% glycerol addition. Similarly, as expected from the previous observations, the sample treated with debonder contains much higher amounts of residual fibres after two and three passes compared to other samples, but drops to similar levels as the others after five passes. These results clearly demonstrate that the debonder disrupts the grinding process, especially with the coarse grinding stones. It is also notable that the sample treated with the choline chloride-glycerol (1:2) DES has significantly more residual fibres than the tap water sample after two and three passes. This would suggest that the choline chloride ions released from the DES complex interfere with the fibrillation of the fibres more than tap water, which is in line with the water retention results, but slightly contradicted by the viscosity results.

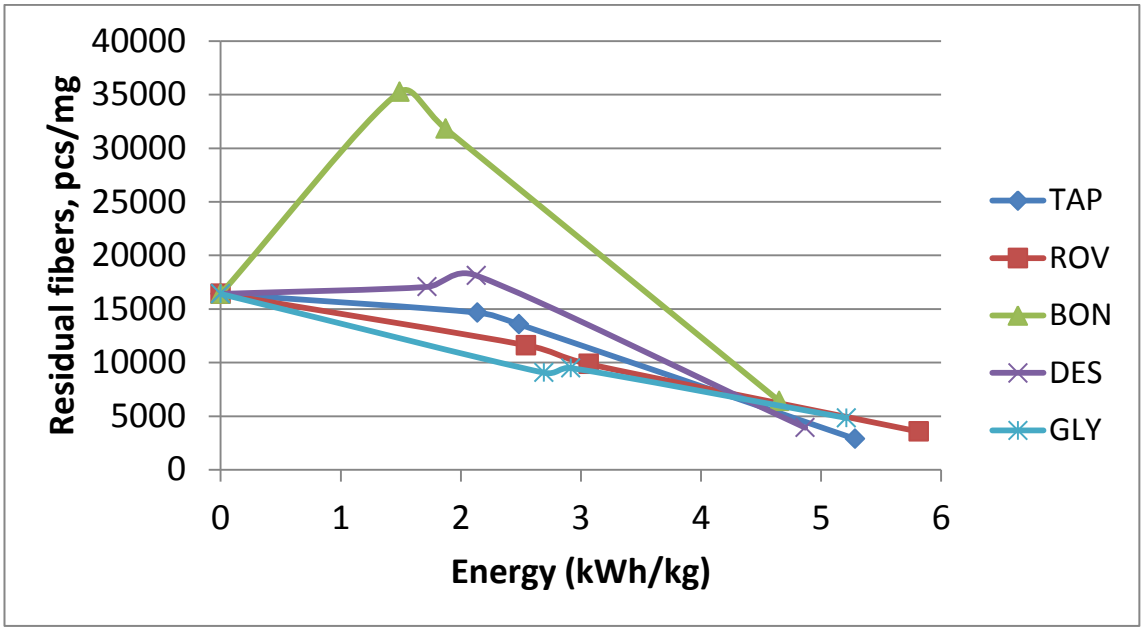

Figure 13. The amount of residual fibres (pieces/mg) on the fibrillated samples as a function of energy consumption during the grinding process. ROV=the control dispersed in RO-water; TAP=sample dispersed in tap water; BON=sample treated with 5% Prosoft debonder; DES=sample treated with 5% choline chloride-glycerol (1:2) deep eutectic solvent; GLY=sample treated with 5% glycerol.

6. CONCLUSIONS FROM EXPERIMENTAL WORK

The aim of this thesis was to provide a systematic outlook on the effect of process conditions, especially the composition of the process medium, on the production of CNF with a Masuko friction grinder. The focus of was on the relationship of the quality of the fibrillated material and the energy used in the grinding process. The study was conducted by optimizing the grinding conditions with trial runs and then performing the test runs with RO-water, tap water and a series of additives. RO-water was used as a control and three additives were used in the study: a Prosoft TQ1003EU cationic oleylimidazoline debonder, glycerol, and a choline chloride-glycerol (1:2) deep eutectic solvent (DES). The effect of tap water and the additives were compared to the RO-water control by performing a series of routine characterization methods found from literature. The results of the characterization methods were presented as a function of

grinding energy to illustrate the relationship between quality and energy demand for each sample.

The results from the characterization methods were very consistent, and clearly demonstrate that the RO-water control generally exhibits the highest levels of fibrillation, viscosity, water retention and dispersion stability. Additionally, the values peak after two or three passes through the grinder, or at energy levels between 2 and 3 kWh/kg, and begin to decrease afterwards. These results indicate that RO-water seems to significantly enhance the swelling of the fibres, resulting in the opening of the fibril bundles and more effective fibrillation. On the other hand, prolonged grinding begins to reduce the aspect ratio of the fibres, leading to the weakening of the interfibrillar network that gives nanocellulose its properties. Overall, the swelling effect of the RO-water on the fibres is the most powerful fibrillation facilitator in this study, and it seems like the most suitable medium for applications such as emulsions where high viscosity, water retention and dispersion stability are desired.

The difference between tap water and RO-water is also significant, suggesting that the divalent cations found in tap water disrupt the swelling of the fibres by reversing the optimal sodium counter-ion form of the fibril surface. The chloride-glycerol (1:2) DES-treated sample behaved mostly similarly as the tap water sample, suggesting that small amounts of the DES do not form a complex structure in an aqueous solution, but instead reverse to choline chloride salt and glycerol, and the former seems to disrupt the fibrillation of the fibres in a similar way as the divalent cations is tap water.

The Prosoft debonder clearly disrupted the fibrillation process, presumably by creating fibril flocks or aggregates around the cationic polymers that are cut to pieces instead of fibrillating properly. The formation of interfibrillar network was also hindered by the formation of these debonder-fibril aggregates. Although the sample fibrillates poorly compared to others, it could be useful in applications where low viscosity and easy water removal are advantageous. The sample treated with glycerol, on the other hand behaves almost exactly like the RO-water control, suggesting that glycerol either has a similar effect on fibrillation as RO-water, or that its effect is small and overshadowed

by the swelling effect of RO-water. In any case it seems not to interfere with the swelling like tap water and the other additives.

Overall, it seems that in most measurements, there is an energy level after which further grinding does not significantly increase the properties of the fibril suspension. The key point is then to detect the minimum level of energy consumption to reach a desired quality threshold, which in this study seems fall be between 2 and 3 kWh/kg for all the samples except for the one treated with debonder for which this point was never reached. However, additional studies with more frequent sampling at the lower grinding energy levels are required to see if the optimal level for RO-water control and glycerol sample that is even below that.

7. SUGGESTIONS FOR FURTHER RESEARCH

Further studies on the effect of the ionic composition of the water on the fibrillation process with dose-response trials are suggested. Namely, the effect of altering the amount of divalent and trivalent cations is of particular interest. Similarly, dose-response trials with glycerol and their effect on fibre fibrillation and especially viscosity are suggested. Additionally, studying the effect of the choline-chloride – glycerol (1:2) deep eutectic solvent as a non-aqueous pre-treatment media that is removed by rinsing is suggested.

8. REFERENCES

Abdul Khalil, H.P.S. et al., 2014. Production and modification of nanofibrillated cellulose using various mechanical processes: A review. *Carbohydrate Polymers*, 99, pp.649–665.

Abdul Khalil, H.P.S., Bhat, A.H. & Ireana Yusra, A.F., 2012. Green composites from sustainable cellulose nanofibrils: A review. *Carbohydrate Polymers*, 87(2), pp.963–979.

Abe, K., Iwamoto, S. & Yano, H., 2007. Obtaining cellulose nanofibers with a uniform

width of 15nm from wood. *Biomacromolecules*, 8, pp.3276–3278.

Abe, K. & Yano, H., 2009. Comparison of the characteristics of cellulose microfibril aggregates isolated from fiber and parenchyma cells of Moso bamboo (Phyllostachys pubescens). *Cellulose*, 17(2), pp.271–277.

Alila, S. et al., 2013. Non-woody plants as raw materials for production of microfibrillated cellulose (MFC): A comparative study. *Industrial Crops and Products*, 41(1), pp.250–259.

Andresen, M. et al., 2007. Nonleaching antimicrobial films prepared from surface-modified microfibrillated cellulose. *Biomacromolecules*, 8(7), pp.2149–2155.

Andresen, M. & Stenius, P., 2007. Water-in-oil Emulsions Stabilized by Hydrophobized Microfibrillated Cellulose. *Journal of Dispersion Science and Technology*, 28(6), pp.837–844.

Ankerfors, M., 2012. *Microfibrillated cellulose: Energy-efficient preparation techniques and key properties*. KTH Royal Institute of Technology.

Bardet, R. & Bras, J., 2014. Cellulose Nanofibers and Their Use in Paper Industry. *Handbook of Green Materials : Processing Technologies, Properties and Applications (In 4 Volumes), Edited by World Scientific*, pp.207–232.

Barnes, H.A. & Nguyen, Q.D., 2001. Rotating vane rheometry-a review. *Journal of Non-Newtonian Fluid Mechanics*, 98(1), pp.1–14.

Benkaddour, A. et al., 2013. Grafting of Polycaprolactone on Oxidized Nanocelluloses by Click Chemistry. *Nanomaterials*, 3(1), pp.141–157.

Bäckström, M. and Hammar, L.-Å., 2010. The influence of the counter-ions to the charged groups in the refinability of never-dried bleached pulps. *BioResources*, 5(2006), pp.2751–2764.

Carrillo, C.A., Laine, J. & Rojas, O.J., 2014. Microemulsion systems for fiber deconstruction into cellulose nanofibrils. *ACS Applied Materials and Interfaces*, 6(24), pp.22622–22627.

Cavaille, J. et al., 2000. Cellulose microfibril-reinforced polymers and their applications. *US Patent 6,103,790*.

Chinga-Carrasco, G., 2013. Optical methods for the quantification of the fibrillation degree of bleached MFC materials. *Micron*, 48, pp.42–48.

Eichhorn, S.J. et al., 2010. Review: Current international research into cellulose nanofibres and nanocomposites. *Journal of Materials Science*, 45(1), pp.1–33.

Eriksen, Ø., Syverud, K. & Gregersen, Ø., 2008. The use of microfibrillated cellulose produced from kraft pulp as strength enhancer in TMP paper. *Nordic Pulp and Paper Research Journal*, 23(03), pp.299–304.

Eronen, P. et al., 2012. Comparison of multilayer formation between different cellulose nanofibrils and cationic polymers. *Journal of colloid and interface science*, 373(1),

pp.84–93.

Fall, A.B., Burman, A. & Wågberg, L., 2014. Cellulosic nanofibrils from eucalyptus , acacia and pine fibers. *Nordic Pulp & Paper Research Journal*, 29(1), pp.176–184.

Fernandes Diniz, J.M.B., Gil, M.H. & Castro, J.A.A.M., 2004. Hornification - Its origin and interpretation in wood pulps. *Wood Science and Technology*, 37(6), pp.489–494.

Goodland, R., 1995. The Concept of Environmental Sustainability. *Annual Review of Ecology and Systematics*, 26(1), pp.1–24.

Gousse, C. et al., 2004. Surface silylation of cellulose microfibrils: Preparation and rheological properties. *Polymer*, 45(5), pp.1569–1575.

Graveson, I. & English, R., 2013. Low energy method for the preparation of non-derivatized nanocellulose. *U.S. Patent Application No. 14/413,449*.

Grignon, J. & Scallan, a. M., 1980. EFFECT OF pH AND NEUTRAL SALTS UPON THE SWELLING OF CELLULOSE GELS. *Journal of Applied Polymer Science*, 25(12), pp.2829–2843.

Habibi, Y., 2014. Key advances in the chemical modification of nanocelluloses. *Chemical Society reviews*, 43(5), pp.1519–42.

Hansen, N.M.L. et al., 2012. Properties of plasticized composite films prepared from nanofibrillated cellulose and birch wood xylan. *Cellulose*, 19(6), pp.2015–2031.

Henriksson, M. et al., 2007. An environmentally friendly method for enzyme-assisted preparation of microfibrillated cellulose (MFC) nanofibers. *European Polymer Journal*, 43(8), pp.3434–3441.

Hentze, H., 2010. From Nanocellulose Science towards Applications. *Developments in advanced biocomposites*, p.71.

Herrick, F.W. et al., 1983. Microfibrillated Cellulose: Morphology and Accessibility. *Journal of Applied Polymer Science: Applied Polymer Symposium*, 37, pp.797–813.

Iotti, M. et al., 2011. Rheological Studies of Microfibrillar Cellulose Water Dispersions. *Journal of Polymers and the Environment*, 19(1), pp.137–145.

Isogai, A., 2013. Wood nanocelluloses: fundamentals and applications as new bio-based nanomaterials. *Journal of Wood Science*, 59(6), pp.449–459.

Iwamoto, S., Nakagaito, A.N. & Yano, H., 2007. Nano-fibrillation of pulp fibers for the processing of transparent nanocomposites. *Applied Physics A*, 89(2), pp.461–466.

Johansson, L.-S. et al., 2011. Experimental evidence on medium driven cellulose surface adaptation demonstrated using nanofibrillated cellulose. *Soft Matter*, 7(22), p.10917.

Josefsson, G. et al., 2013. Prediction of elastic properties of nanofibrillated cellulose from micromechanical modeling and nano-structure characterization by transmission electron microscopy. *Cellulose*, 20(2), pp.761–770.

Junka, K. et al., 2013. Titrimetric methods for the determination of surface and total charge of functionalized nanofibrillated/microfibrillated cellulose (NFC/MFC). *Cellulose*, 20(6), pp.2887–2895.

Kajanto, I. & Kosonen, M., 2012. The potential use of micro-and nanofibrillated cellulose as a reinforcing element in paper. *Journal of Science & Technology for Forest Products and Processes*, 2(6), pp.42–48.

Kangas, H. et al., 2014. Characterization of fibrillated celluloses. A short review and evaluation of characteristics with a combination of methods. *Nordic Pulp & Paper Research Journal*, 29(1), pp.129 – 143.

Kangas, H., 2014. Opas selluloosa-nanomateriaaleihin. *VTT*. Available at: http://www.vtt.fi/inf/pdf/technology/2014/t199.pdf.

Kleinschmidt, D.C. et al., 1988. Filling-containing, dough-based products containing cellulosic fibrils and microfibrils. *US Patent US 4774095 A*, p.11.

Klemm, D. et al., 2005. Cellulose: fascinating biopolymer and sustainable raw material. *Angewandte Chemie - International Edition*, 44(22), pp.3358–93.

Klemm, D. et al., 2011. Nanocelluloses: A New Family of Nature-Based Materials. *Angewandte Chemie International Edition*, 50(24), pp.5438–5466.

Kolakovic, R. et al., 2012. Nanofibrillar cellulose films for controlled drug delivery. *European journal of pharmaceutics and biopharmaceutics : official journal of Arbeitsgemeinschaft für Pharmazeutische Verfahrenstechnik e.V*, 82(2), pp.308–15.

Korhonen, J.T. et al., 2011. Hydrophobic nanocellulose aerogels as floating, sustainable, reusable, and recyclable oil absorbents. *ACS Applied Materials and Interfaces*, 3(6), pp.1813–1816.

Lahtinen, P. et al., 2014. A Comparative study of fibrillated fibers from different mechanical and chemical pulps. *BioResources*, 9, pp.2115–2127.

Lavoine, N. et al., 2012. Microfibrillated cellulose – Its barrier properties and applications in cellulosic materials: A review. *Carbohydrate Polymers*, 90(2), pp.735–764.

Lee, S.H. et al., 2010. Enzymatic saccharification of woody biomass micro/nanofibrillated by continuous extrusion process II: Effect of hot-compressed water treatment. *Bioresource Technology*, 101(24), pp.9645–9649.

Leppänen, K. et al., 2010. Small-angle x-ray scattering study on the structure of microcrystalline and nanofibrillated cellulose. *Journal of Physics: Conference Series*, 247(1), p.012030.

Lin, L., Yamaguchi, H. & Suzuki, A., 2013. Dissolution of cellulose in the mixed solvent of bmim]Cl-DMAc and its application. *RSC Advances*, 3(34), pp.14379–14384.

Lindström, T. et al., 2014. The Emergence of Practical Nanocellulose Applications For A More Sustainable Paper / Board Industry. *Indian Pulp and Paper Technical*

Association Journal, 26(1), pp.53–61.

Lindström, T. & Carlsson, G., 1982. The effect of chemical environment on fiber swelling. *Svensk Papperstindning-Nordisk Cellulosa*, 85(3), pp.R14–R20.

Liu, H. et al., 2009. Visualization of enzymatic hydrolysis of cellulose using AFM phase imaging. *Enzyme and Microbial Technology*, 45(4), pp.274–281.

Lönnberg, H. et al., 2011. Synthesis of polycaprolactone-grafted microfibrillated cellulose for use in novel bionanocomposites-influence of the graft length on the mechanical properties. *ACS Applied Materials and Interfaces*, 3(5), pp.1426–1433.

Mautner, A. et al., 2014. Nanopapers for organic solvent nanofiltration. *Chem Commun (Camb)*, 50(43), pp.5778–5781.

Mondet, J., 1999. Cosmetic use of natural microfibrils and a film-forming polymer as a composite coating agent for hair, eyelashes, eyebrows and nails. *US Patent 6,001,338*.

Moon, R.J. et al., 2011. Cellulose nanomaterials review: structure, properties and nanocomposites. *Chem Soc Rev*, 40(7), pp.3941–3994.

Moon, R.J., Pohler, T. & Tammelin, T., 2014. Microscopic Characterization of Nanofibers and Nanocrystals. *Handbook of Green Materials, Vol 1: Bionanomaterials: Separation Processes, Characterization and Properties*, 5, pp.159–180.

Nishiyama, Y. et al., 2003. Crystal structure and hydrogen bonding system in cellulose Iα from synchrotron X-ray and neutron fiber diffraction. *J. Am. Chem. Soc.*, 125, pp.14300–14306.

de Nooy, a. E.J. et al., 1996. TEMPO-Mediated Oxidation of Pullulan and Influence of Ionic Strength and Linear Charge Density on the Dimensions of the Obtained Polyelectrolyte Chains. *Macromolecules*, 29(20), pp.6541–6547.

Okahisa, Y. et al., 2009. Optically transparent wood – cellulose nanocomposite as a base substrate for flexible organic light-emitting diode displays. *Composites Science and Technology*, 69(11-12), pp.1958–1961.

Orelma, H. et al., 2012. Surface functionalized nanofibrillar cellulose (NFC) film as a platform for immunoassays and diagnostics. *Biointerphases*, 7(1-4), pp.1–12.

Osong, S.H., Norgren, S. & Engstrand, P., 2015. Processing of wood-based microfibrillated cellulose and nanofibrillated cellulose, and applications relating to papermaking: a review. *Cellulose*.

Pajari, H., Rautkoski, H. & Moilanen, P., 2012. Replacement of synthetic binders with nanofibrillated cellulose in board coating: pilot scale studies. *APPI international conference on nanotechnology for revenwable materials*.

Paltakari, J. et al., 2012. Method for producing modified cellulose. *U.S. Patent Application No. 13/147,346*, 1(19).

Percival Zhang, Y.H., Himmel, M.E. & Mielenz, J.R., 2006. Outlook for cellulase improvement: Screening and selection strategies. *Biotechnology Advances*, 24(5), pp.452–481.

Peresin, M.S. et al., 2014. Exploring alternative raw materials sources for nanocellulose production. , pp.1–5.

Pääkko, M. et al., 2007. Enzymatic hydrolysis combined with mechanical shearing and high-pressure homogenization for nanoscale cellulose fibrils and strong gels. *Biomacromolecules*, 8(6), pp.1934–1941.

Pöhler, T. et al., 2010. Influence of fibrillation method on the character of nanofibrillated cellulose (NFC). In *TAPPI International Conference on Nanotechnology for the ForestProduct Industry*. pp. 437–458.

Rouilly, a., Geneau-Sbartaï, C. & Rigal, L., 2009. Thermo-mechanical processing of sugar beet pulp. III. Study of extruded films improvement with various plasticizers and cross-linkers. *Bioresource Technology*, 100(12), pp.3076–3081.

Saito, T. et al., 2006. Homogeneous suspensions of individualized microfibrils from TEMPO-catalyzed oxidation of native cellulose. *Biomacromolecules*, 7(6), pp.1687–1691.

Scallan, A.M. & Grignon, J., 1979. The effect of cations on pulp and paper properties. *Svensk papperstidning*, (2), pp.40–47.

Sehaqui, H. et al., 2010. Mechanical performance tailoring of tough ultra-high porosity foams prepared from cellulose I nanofiber suspensions. *Soft Matter*, 6(8), p.1824.

Sehaqui, H. et al., 2011. Strong and tough cellulose nanopaper with high specific surface area and porosity. *Biomacromolecules*, 12(10), pp.3638–44.

Shatkin, J.O.A., Wegner, T.H. & Bilek, E.M.T.E.D., 2014. Nanocellulose Markets. *Tappi Journal*, 13(5), pp.9–16.

Siqueira, G., Bras, J. & Dufresne, A., 2010. New process of chemical grafting of cellulose nanoparticles with a long chain isocyanate. *Langmuir*, 26(1), pp.402–411.

Siró, I. & Plackett, D., 2010. Microfibrillated cellulose and new nanocomposite materials: a review. *Cellulose*, 17(3), pp.459–494.

Sirviö, J.A., Visanko, M. & Liimatainen, H., 2015. Deep eutectic solvent system based on choline chloride-urea as a pre-treatment for nanofibrillation of wood cellulose. *Green Chem.*, 17(6), pp.3401–3406.

Spence, K.L. et al., 2011. A comparative study of energy consumption and physical properties of microfibrillated cellulose produced by different processing methods. *Cellulose*, 18(4), pp.1097–1111.

Spence, K.L., Venditti, R.A., Habibi, Y., et al., 2010. The effect of chemical composition on microfibrillar cellulose films from wood pulps: Mechanical processing and physical properties. *Bioresource Technology*, 101(15), pp.5961–5968.

Spence, K.L., Venditti, R.A., Rojas, O.J., et al., 2010. The effect of chemical composition on microfibrillar cellulose films from wood pulps: water interactions and physical properties for packaging applications. *Cellulose*, 17(4), pp.835–848.

Spiridon, I. & Popa, V.I., 2000. Application of microorganisms and enzymes in the pulp and paper industry. *Cellulose Chemistry and Technology*, 34(3-4), pp.275–285.

Suzuki, M. & Mori, S., 2003. Highly absorbent composite sheets and methods of manufacturing the same. *US Patent App. 10/357,232*.

Taipale, T. et al., 2010. Effect of microfibrillated cellulose and fines on the drainage of kraft pulp suspension and paper strength. *Cellulose*, 17(5), pp.1005–1020.

Takai, H. & Konishi, T., 2004. Water-disintegratable sheet and manufacturing method thereof. *US Patent 6,749,718*.

Tammelin, T., Hippi, U. & Salminen, A., 2013. Method for the preparation of nfc films on supports. *US Patent App. 14/353,775*.

Tanaka, A. et al., 2012. Nanocellulose characterization with mechanical fractionation. *Nordic Pulp and Paper Research Journal*, 27(04), pp.689–694.

Taniguchi, T. & Okamura, K., 1998. New films produced from microfibrillated natural fibres. *Polymer International*, 47(3), pp.291–294.

Tingaut, P., Hauert, R. & Zimmermann, T., 2011. Highly efficient and straightforward functionalization of cellulose films with thiol-ene click chemistry. *Journal of Materials Chemistry*, 21(40), p.16066.

Tollefson, J. & Weiss, K.R., 2015. Nations adopt historic global climate accord. *Nature*, 528(7582), pp.315–316.

Turbak, A., Snyder, F. & Sandberg, K., 1985. Suspensions containing microfibrillated cellulose. *US Patent 4,500,546*.

Walecka, Jerrold, A., 1956. An investigation of low degree of substitution carboxymethylcelluloses. *Doctoral dissertation. Lawrence College, Institute of Paper Chemistry. Retrieved from http://smartech.gatech.edu/handle/1853/5696*, (39), p.458.

Wang, Q.Q. et al., 2012. Morphological development of cellulose fibrils of a bleached eucalyptus pulp by mechanical fibrillation. *Cellulose*, 19, pp.1631–1643.

Vartiainen, J., Kaljunen, T. & Nykänen, H., 2014. Improving multilayer packaging performance with nanocellulose barrier layer. *TAPPI Place Conference*.

Weibel, M., 2001. Use of structurally expanded cellulose to enhance the softness and retard staling of baked products. *US Patent 6,251,458*.

Wicklein, B. et al., 2015. Thermally insulating and fire-retardant lightweight anisotropic foams based on nanocellulose and graphene oxide. *Nature nanotechnology*, 10(3), pp.277–83.

Viikari, L. et al., 2007. *Thermostable enzymes in lignocellulose hydrolysis* L. Olsson, ed.,

Berlin, Heidelberg: Springer Berlin Heidelberg.

Williamson, M., 2015. Microfibrils set to transform paper furnish. *TAPPI Paper360 - March/April 2015*, pp.56–58.

Wågberg, L. et al., 1987. On the charge stoichiometry upon adsorption of a cationic polyelectrolyte on cellulosic materials. *Colloids and Surfaces*.

Wågberg, L. et al., 2008. The build-up of polyelectrolyte multilayers of microfibrillated cellulose and cationic polyelectrolytes. *Langmuir*, 24(3), pp.784–795.

Xhanari, K. et al., 2011. Reduction of water wettability of nanofibrillated cellulose by adsorption of cationic surfactants. *Cellulose*, 18(2), pp.257–270.

Yaginuma, Y., Mochihara, N. & Tanaka, Y., 2010. Water-dispersible cellulose and process for producing the same. *US Patent WO 2004007558 A1*.

Yang, Y. et al., 2005. Conductive carbon nanofiber-polymer foam structures. *Advanced Materials*, 17(16), pp.1999–2003.

Zheng, H., 2014. Production of fibrillated cellulose materials - effects of pretreatments and refining strategy on pulp properties. *Master's thesis. Aalto University, school of chemical technology. Retrieved from Aaltodoc: http://urn.fi/URN:NBN:fi:aalto-201405131808*.

Zhu, H. et al., 2012. A Novel Nano Cellulose Preparation Method and Size Fraction by Cross Flow Ultra- Filtration. *Current Organic Chemistry*, 16(16), pp.1871–1875.

Österberg, M. et al., 2013. A fast method to produce strong NFC films as a platform for barrier and functional materials. *ACS Applied Materials and Interfaces*, 5(11), pp.4640–4647.

APPENDIX

Appendix 1 Results from characterization methods

Results from the viscosity measurements. ROV=the control dispersed in RO-water; TAP=sample dispersed in tap water; BON=sample treated with 5% Prosoft debonder; DES=sample treated with 5% choline chloride-glycerol (1:2) deep eutectic solvent; GLY=sample treated with 5% glycerol. The number after the sample name denotes the number of passes through the grinder.

Sample	Spindle	Yield value	StDev	95% Confidence	Viscosity 10 rpm (Pa*s)	StDev	95% Confidence
ROV2	V75	175,9	0,5	0,6	104455,2	2104,3	2916,3
ROV3	V75	142,1	0,3	0,4	80450,1	2335,6	3236,9
ROV5	V75	89,9	1,7	2,4	57190,5	1010,3	1400,2
TAP2	V73	79,7	1,0	1,4	29237,8	528,0	731,7
TAP3	V73	74,5	4,3	6,0	30254,3	1436,7	1991,2
TAP5	V73	62,3	0,5	0,7	30896,3	167,8	232,5
BON2	V73	58,3	0,1	0,2	9902,9	359,7	498,6
BON3	V73	60,6	0,8	1,1	13947,5	892,4	1236,8
BON5	V73	76,5	10,2	14,1	36112,5	425,8	590,1
DES2	V73	73,6	4,6	6,3	29960,0	1514,5	2098,9
DES3	V73	85,8	6,3	8,8	33180,7	801,4	1110,7
DES5	V73	63,0	6,6	9,2	29895,8	1039,5	1440,6
GLY2	V75	161,6	3,3	4,5	89396,1	803,6	1113,7
GLY3	V75	142,5	1,4	2,0	78320,1	2181,6	3023,4
GLY5	V75	98,9	0,3	0,4	59064,9	1238,1	1715,9

Results from the gravimetric water retention measurements. ROV=the control dispersed in RO-water; TAP=sample dispersed in tap water; BON=sample treated with 5% Prosoft debonder; DES=sample treated with 5% choline chloride-glycerol (1:2) deep eutectic solvent; GLY=sample treated with 5% glycerol; Zero=unfibrillated fibre suspension. The number after the sample name denotes the number of passes through the grinder.

Sample	Water removed (g)	Sample size (ml)	Solids content of sample (%)	Water removed (%)	Water retention value (g/g)	StDev	95% Confidence
ROV2	0,9	3,0	0,21	0,3	329,7	3,1	3,5
ROV3	0,9	3,0	0,20	0,3	346,2	7,6	7,5
ROV5	0,9	3,0	0,20	0,3	344,8	1,4	1,6
TAP2	2,3	3,0	0,21	0,8	122,2	23,9	23,5
TAP3	1,4	3,0	0,20	0,5	263,0	1,9	2,2
TAP5	1,2	3,0	0,20	0,4	298,2	5,4	5,3
BON2	2,9	3,0	0,20	1,0	16,5	5,2	5,9
BON3	2,9	3,0	0,21	1,0	22,5	13,1	12,8
BON5	2,1	3,0	0,20	0,7	146,9	20,0	22,7
DES2	2,2	3,0	0,20	0,7	130,5	17,8	15,6
DES3	1,8	3,0	0,21	0,6	202,2	11,1	12,6
DES5	1,5	3,0	0,20	0,5	246,8	26,1	25,6
GLY2	0,9	3,0	0,20	0,3	344,4	8,4	8,2
GLY3	0,8	3,0	0,20	0,3	360,6	3,5	3,4
GLY5	0,8	3,0	0,21	0,3	344,5	1,7	2,0
Zero	3,0	3,0	0,21	1,0	7,7	5,0	5,7

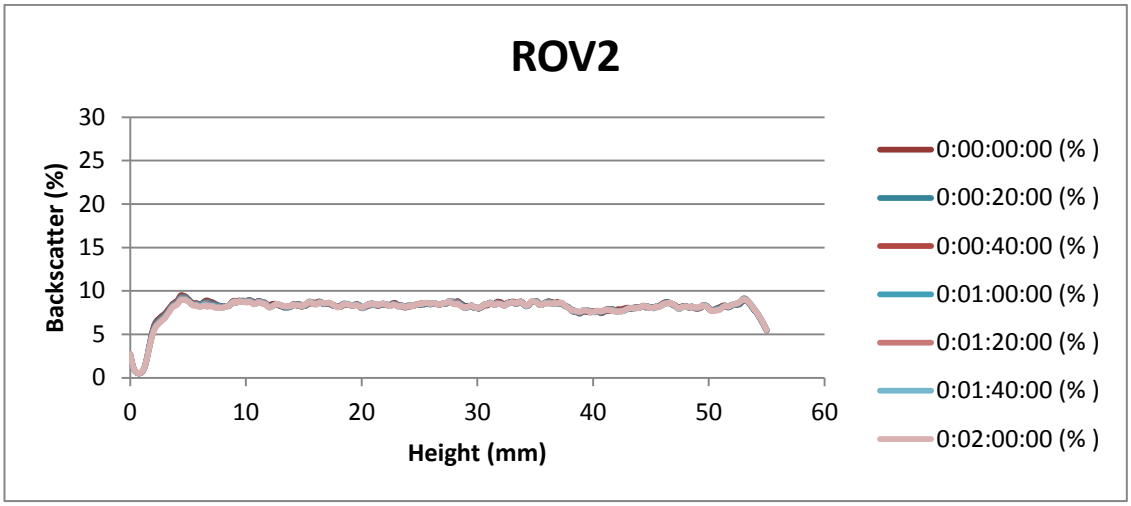

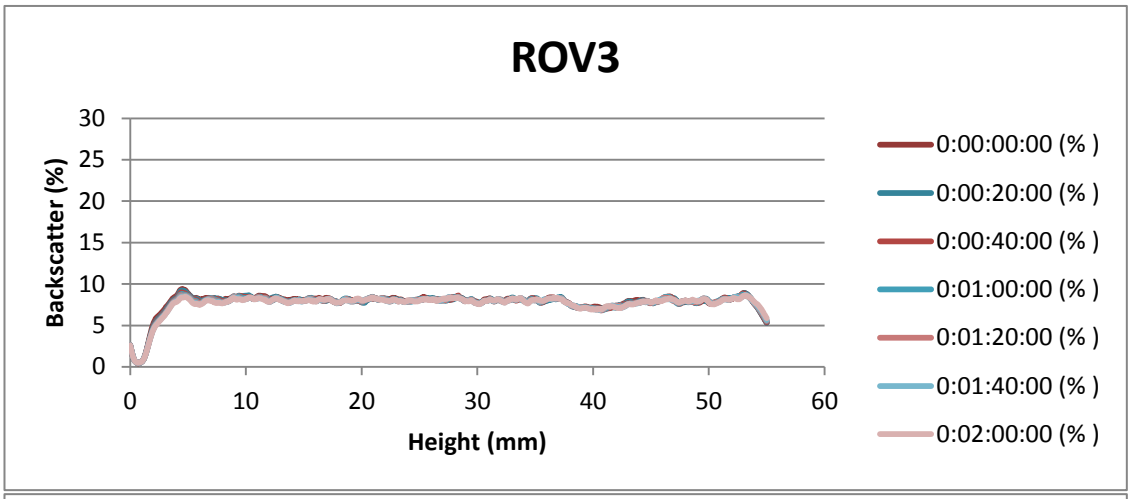

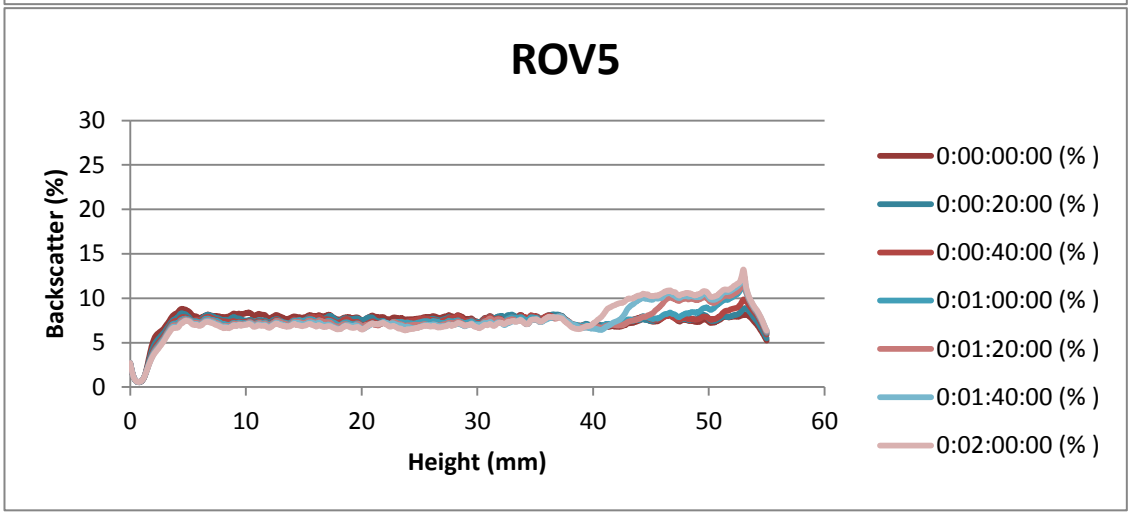

The backscatter (%) of the control treated with RO-water after two, three and five passes through the grinder, respectively, presented as a function of the height of the sample. The measurements were performed with TurbiScan LAB instrument at every five minutes for two hours, and the measurements of every 20 minutes are presented in the chart.

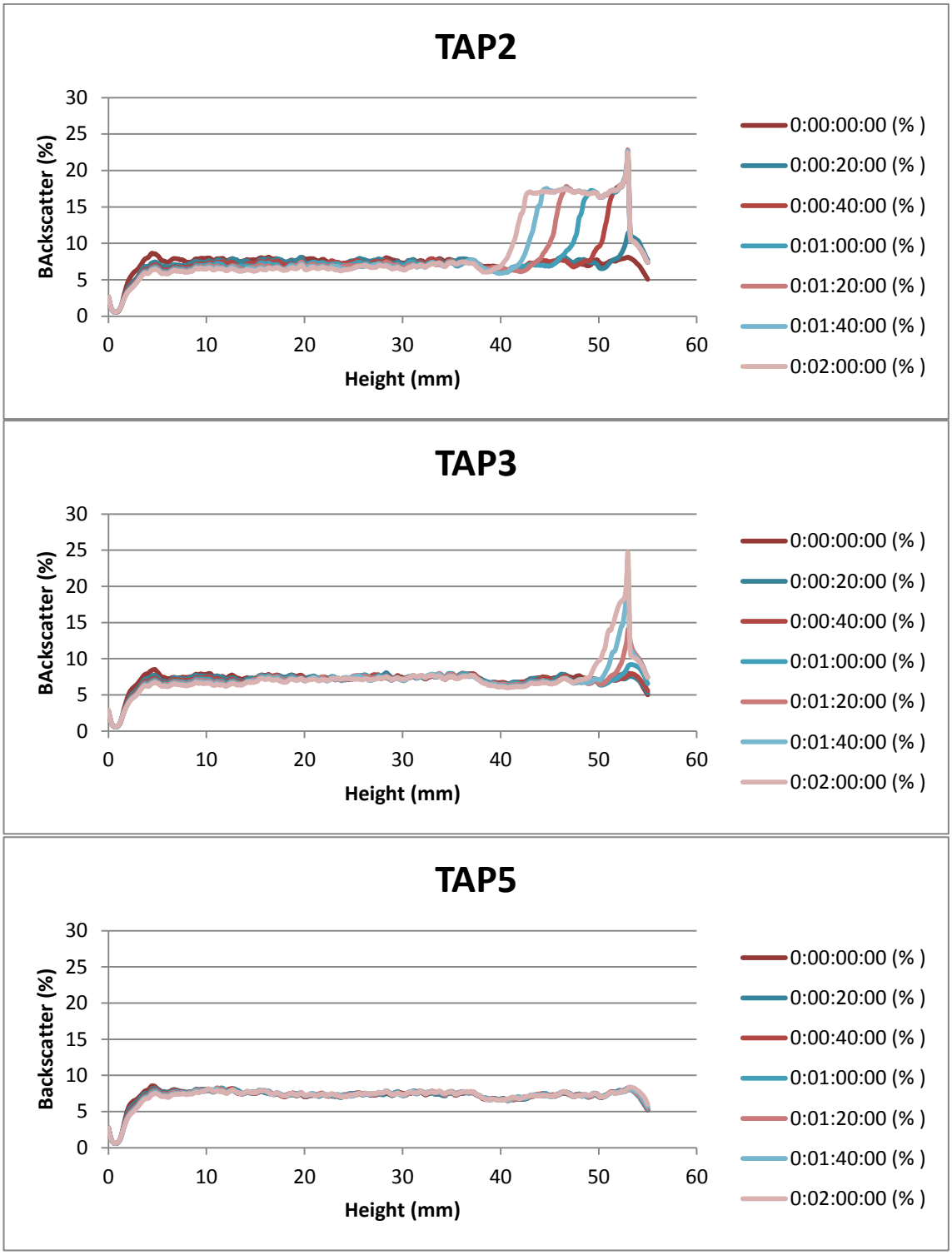

The backscatter (%) of the sample treated with tap water after two, three and five passes through the grinder, respectively, presented as a function of the height of the sample. The measurements were performed with TurbiScan LAB instrument at every five minutes for two hours, and the measurements of every 20 minutes are presented in the chart.

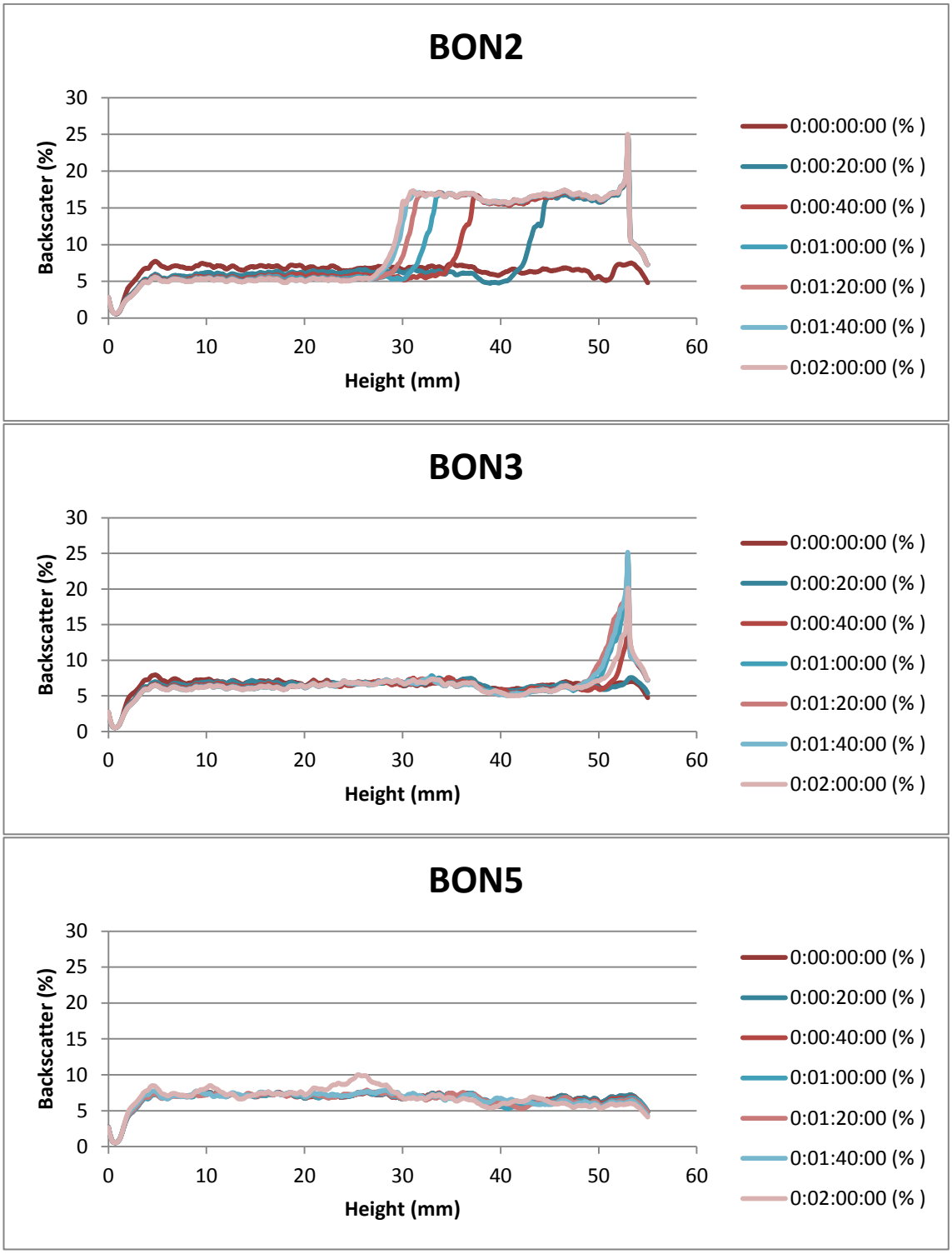

The backscatter (%) of the sample treated with 5% Prosoft debonder after two, three and five passes through the grinder, respectively, presented as a function of the height of the sample. The measurements were performed with TurbiScan LAB instrument at every five minutes for two hours, and the measurements of every 20 minutes are presented in the chart.

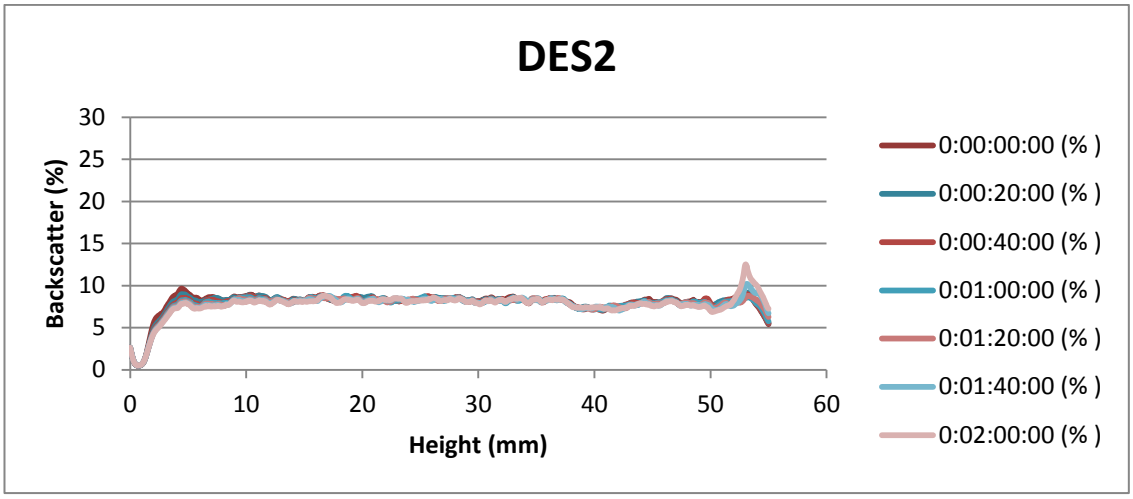

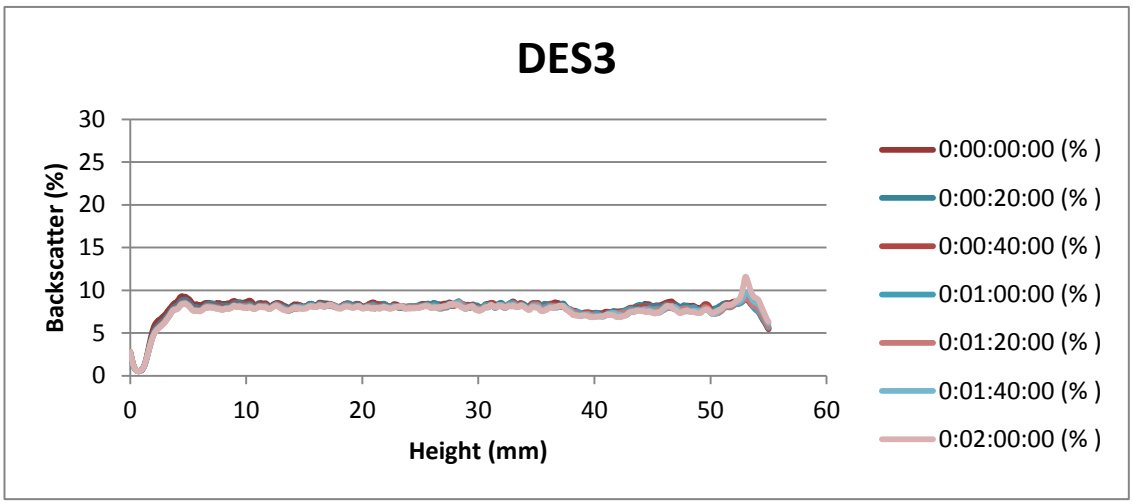

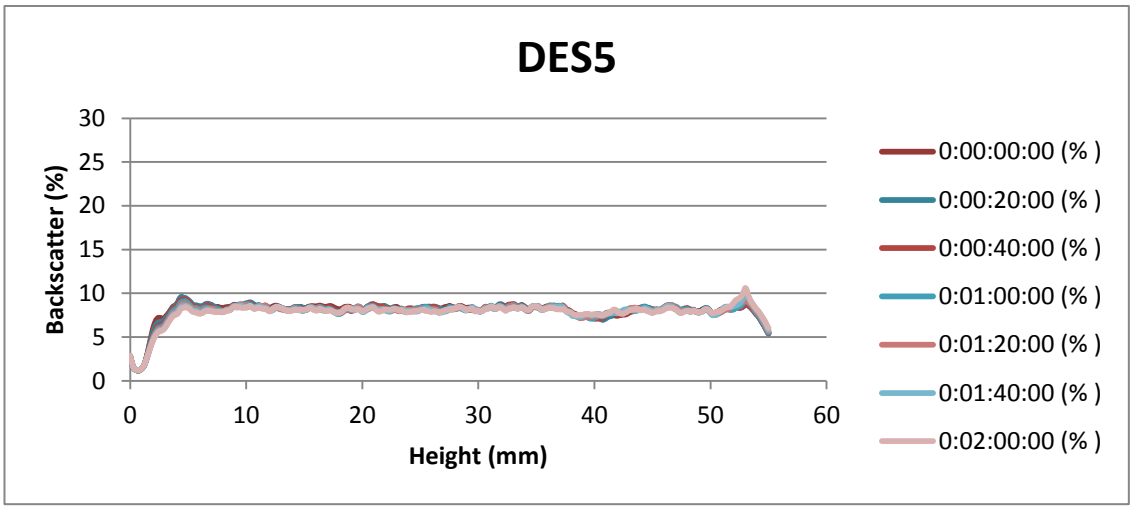

The backscatter (%) of the sample treated with 5% choline chloride-glycerol (1:2) deep eutectic solvent after two, three and five passes through the grinder, respectively, presented as a function of the height of the sample. The measurements were performed with TurbiScan LAB instrument at every five minutes for two hours, and the measurements of every 20 minutes are presented in the chart.

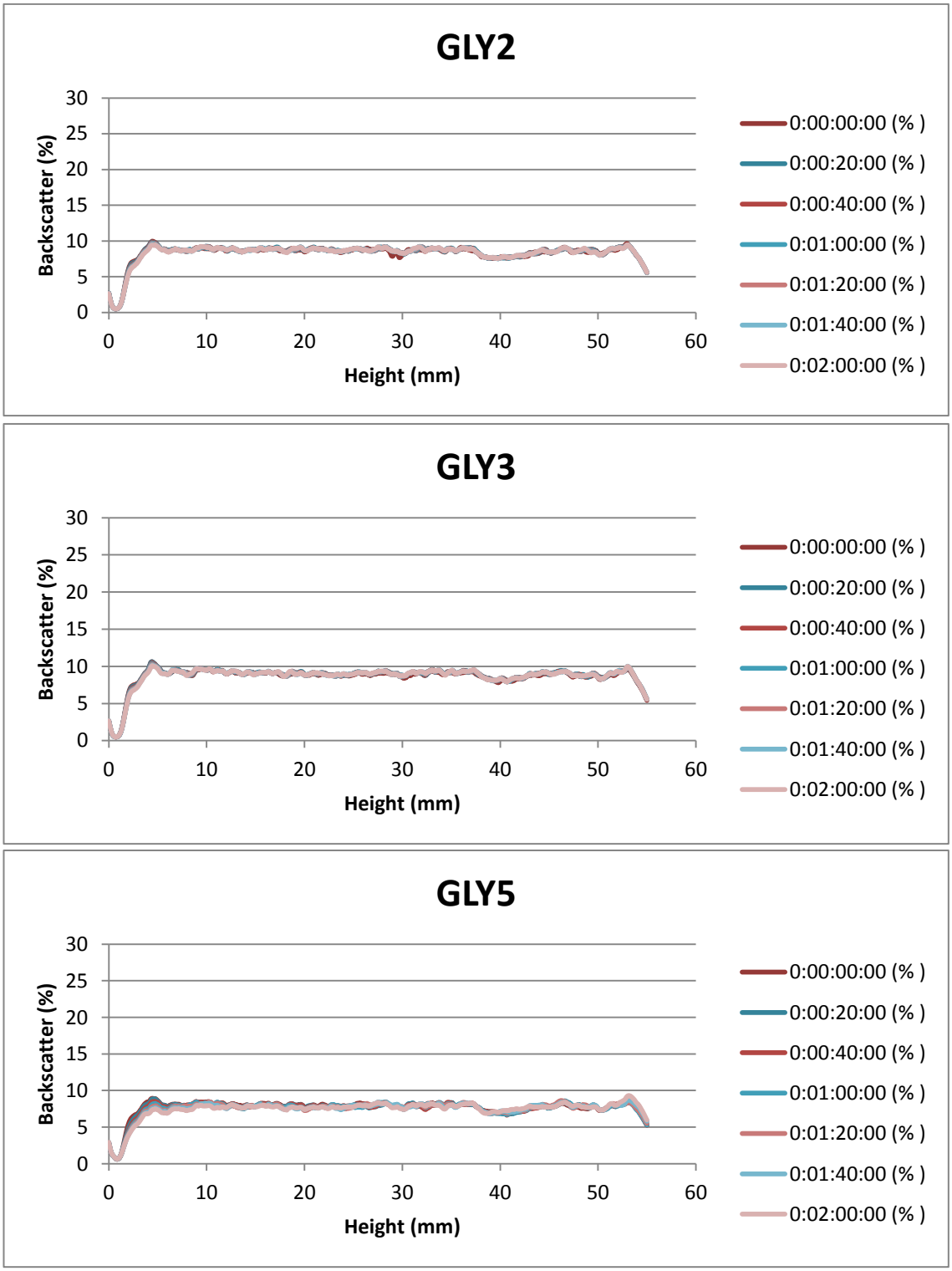

The backscatter (%) of the sample treated with 5% glycerol after two, three and five passes through the grinder, respectively, presented as a function of the height of the sample. The measurements were performed with TurbiScan LAB instrument at every five minutes for two hours, and the measurements of every 20 minutes are presented in the chart.

ΔH values from the TurbiScan backscatter measurements. The values represent the change of the height of the sediment at given time, compared to the original height of the sediment at 0sec. ROV=the control dispersed in RO-water; TAP=sample dispersed in tap water; BON=sample treated with 5% Prosoft debonder; DES=sample treated with 5% choline chloride-glycerol (1:2) deep eutectic solvent; GLY=sample treated with 5% glycerol; Zero=unfibrillated fibre suspension. The number after the sample name denotes the number of passes through the grinder.

DeltaH(t) From Backscattering															
t(sec)	ROV2	ROV3	ROV5	TAP2	TAP3	TAP5	BON2	BON3	BON5	DES2	DES3	DES5	GLY2	GLY3	GLY5
0	0,0	0,0	0,0	0,0	0,0	0,0	0,0	0,0	0,0	0,0	0,0	0,0	0,0	0,0	0,0
300	0,0	0,0	0,0	0,0	0,0	0,0	0,0	0,0	0,0	0,0	0,0	0,0	0,0	0,0	0,0
600	0,0	0,0	0,0	0,0	0,0	0,0	3,6	0,0	0,0	0,0	0,0	0,0	0,0	0,0	0,0
900	0,0	0,0	0,0	0,0	0,0	0,0	6,8	0,0	0,0	0,0	0,0	0,0	0,0	0,0	0,0
1200	0,0	0,0	0,0	0,0	0,0	0,0	9,8	0,0	0,0	0,0	0,0	0,0	0,0	0,0	0,0
1500	0,0	0,0	0,0	0,4	0,0	0,0	11,8	0,0	0,0	0,0	0,0	0,0	0,0	0,0	0,0
1800	0,0	0,0	0,0	1,0	0,0	0,0	13,8	0,0	0,0	0,0	0,0	0,0	0,0	0,0	0,0
2100	0,0	0,0	0,0	1,7	0,0	0,0	15,4	0,1	0,0	0,0	0,0	0,0	0,0	0,0	0,0
2400	0,0	0,0	0,2	2,4	0,0	0,0	16,7	0,3	0,0	0,0	0,0	0,0	0,0	0,0	0,0
2700	0,0	0,0	0,6	3,1	0,0	0,0	17,5	0,6	0,0	0,0	0,0	0,0	0,0	0,0	0,0
3000	0,0	0,0	1,2	3,9	0,0	0,0	18,7	1,1	0,0	0,0	0,0	0,0	0,0	0,0	0,0
3300	0,0	0,0	1,9	4,6	0,0	0,0	19,5	1,4	0,0	0,0	0,0	0,0	0,0	0,0	0,0
3600	0,0	0,0	2,8	5,2	0,0	0,0	20,2	1,8	0,0	0,0	0,0	0,0	0,0	0,0	0,0
3900	0,0	0,0	4,5	5,8	0,0	0,0	20,9	2,1	0,0	0,0	0,0	0,0	0,0	0,0	0,0
4200	0,0	0,0	5,6	6,4	0,0	0,0	21,4	2,3	0,0	0,0	0,0	0,0	0,0	0,0	0,0
4500	0,0	0,0	6,5	7,0	0,0	0,0	21,9	2,3	0,0	0,0	0,0	0,0	0,0	0,0	0,0
4800	0,0	0,0	7,3	7,5	0,2	0,0	22,2	2,4	0,0	0,0	0,0	0,0	0,0	0,0	0,0
5100	0,0	0,0	8,0	8,1	0,3	0,0	22,5	2,4	0,0	0,1	0,0	0,0	0,0	0,0	0,0
5400	0,0	0,0	8,6	8,6	0,5	0,0	22,8	2,3	0,0	0,7	0,0	0,0	0,0	0,0	0,0
5700	0,0	0,0	9,5	9,2	0,8	0,0	23,0	2,1	0,0	0,9	0,0	0,3	0,0	0,0	0,0
6000	0,0	0,0	10,2	9,7	1,1	0,0	23,1	2,1	0,0	1,1	1,8	0,5	0,0	0,0	0,0
6300	0,0	0,0	10,7	10,2	1,5	0,0	23,3	1,9	0,0	2,0	2,0	0,7	0,0	0,0	0,0
6600	0,0	0,0	11,2	10,6	1,7	0,0	23,4	1,7	3,6	2,1	2,1	0,9	0,0	0,0	0,0
6900	0,0	0,0	11,7	11,0	2,0	0,0	23,4	1,2	5,1	2,2	2,2	1,0	0,0	0,0	0,6
7200	0,0	0,0	12,1	11,4	2,4	0,0	23,5	0,9	7,3	2,3	2,3	1,1	0,0	0,0	0,7

Results from the Fibrelab analyser. ROV=the control dispersed in RO-water; TAP=sample dispersed in tap water; BON=sample treated with 5% Prosoft debonder; DES=sample treated with 5% choline chloride-glycerol (1:2) deep eutectic solvent; GLY=sample treated with 5% glycerol; Zero=unfibrillated fibre suspension. The number after the sample name denotes the number of passes through the grinder.

Sample	Weight (mg)	Fibers measured (pcs)	Fibers/mg (pcs/mg)	Average (pcs/mg)	StDev	95% Confidence
ROV2	2,00	22159	11091,1	11868,2	1098,9	1523,0
	2,00	25264	12645,3			
ROV3	2,04	19984	9791,3	9861,1	98,7	136,8
	2,04	20269	9930,9			
ROV5	2,08	7259	3489,9	3559,4	98,2	136,2
	2,08	7548	3628,8			
TAP2	2,02	29175	14414,5	14663,0	351,5	487,1
	2,02	30181	14911,6			
TAP3	2,03	27619	13605,4	13573,9	44,6	61,8
	2,03	27491	13542,4			
TAP5	2,01	5933	2947,3	2875,3	101,9	141,2
	2,01	5643	2803,3			
BON2	2,21	78334	35477,4	35255,7	313,5	434,5
	2,21	77355	35034,0			
BON3	2,09	66167	31734,8	31813,7	111,6	154,6
	2,09	66496	31892,6			
BON5	2,02	12928	6412,7	6404,5	11,6	16,0
	2,02	12895	6396,3			
DES2	2,15	34464	16007,4	17064,1	1494,4	2071,0
	2,15	39014	18120,8			
DES3	2,02	35710	17722,1	18123,3	567,4	786,4
	2,02	37327	18524,6			
DES5	2,00	7988	3998,0	3923,4	105,5	146,2
	2,00	7690	3848,8			
GLY2	2,05	18198	8864,1	9056,0	271,4	376,1
	2,05	18986	9247,9			
GLY3	2,10	20190	9628,0	9487,4	198,9	275,7
	2,10	19600	9346,7			
GLY5	2,08	10329	4961,1	4831,9	182,7	253,2
	2,08	9791	4702,7			
Zero	1,99	32671	16458,9	16410,6	68,4	94,8
	1,99	32479	16362,2			